2018

INVESTIGATION ON CYCLIC VARIATION OF LOW TEMPERATURE COMBUSTION SRATEGIES

Geraint Andrew Howard Bryden
University of Windsor

INVESTIGATION ON CYCLIC VARIATION OF LOW TEMPERATURE COMBUSTION STRATEGIES

by

Geraint Bryden

A Thesis
Submitted to the Faculty of Graduate Studies
through Mechanical, Automotive, and Materials Engineering
in Partial Fulfillment of the Requirements for
the Degree of Master of Applied Science
at the University of Windsor

Windsor, Ontario, Canada

INVESTIGATION ON CYCLIC VARIATION OF LOW TEMPERATURE COMBUSTION STRATEGIES

by

Geraint Bryden

APPROVED BY:

_____

X. Xu

Department of Civil and Environmental Engineering

_____

J. Tjong

Department of Mechanical, Automotive, and Materials Engineering

_____

G. T. Reader, Co-Advisor

Department of Mechanical, Automotive, and Materials Engineering

_____

M. Zheng, Co-Advisor

Department of Mechanical, Automotive, and Materials Engineering

November 13th 2017

AUTHOR'S DECLARATION OF ORIGINALITY

I hereby certify that I am the sole author of this thesis and that no part of this thesis has been published or submitted for publication.

I certify that, to the best of my knowledge, my thesis does not infringe upon anyone's copyright nor violate any proprietary rights and that any ideas, techniques, quotations, or any other material from the work of other people included in my thesis, published or otherwise, are fully acknowledged in accordance with the standard referencing practices. Furthermore, to the extent that I have included copyrighted material that surpasses the bounds of fair dealing within the meaning of the Canada Copyright Act, I certify that I have obtained a written permission from the copyright owner(s) to include such material(s) in my thesis and have included copies of such copyright clearances to my appendix.

I declare that this is a true copy of my thesis, including any final revisions, as approved by my thesis committee and the Graduate Studies office, and that this thesis has not been submitted for a higher degree to any other University or Institution.

ABSTRACT

With increasingly stringent emission standards it is necessary to develop new methods of emission reduction in the internal combustion engine. With the addition of fuel efficiency requirements being added by 2020 the diesel engine is an attractive option for heavy duty applications, due to its greater thermal efficiency compared to its gasoline counterpart. However, diesel engines require a combination of in-cylinder emission reduction and after-treatment devices in order to meet the current emission regulations, but with the implementation of these in-cylinder emission reducing strategies there may be an increase in cyclic variation of combustion. This cyclic variation can cause issues as extreme as misfire, or catastrophic failure from excessive cylinder pressure, or lesser issues such as increased noise or periodic decreases in efficiency. This study investigated the combustion stability of diesel single shot combustion and ethanol port fuel injection and diesel direct injection combustion. The effect of exhaust gas recirculation and combustion phasing on the cycle-to-cycle variation of diesel single shot combustion, and the effect of exhaust gas recirculation and diesel – ethanol ratio on the combustion stability of ethanol port fuel injection with diesel direction is reported. It was found that exhaust gas recirculation did not cause a significant increase in the COV_{IMEP} for the majority of the tests carried out, the exceptions were for tests with over 95% of the fuel energy provided by ethanol port injection. The standard deviation of CA50 increased with the application of EGR, retarding of combustion phasing for diesel single shot combustion, and diesel – ethanol dual fuel combustion.

DEDICATION

I dedicate this thesis to my parents Fiona and Paul, and my girlfriend Katrina for their continual support and effort to help me complete this work.

ACKNOWLEDGEMENTS

Firstly, I would to thank my advisors, Dr Ming Zheng and Dr. Graham Reader for their continuous support and guidance during my time in the Master's program, as well as the opportunity to work in the Clean Combustion Engine Laboratory. I would also like to thank Dr. Jimi Tjong for his support and advice, and for allowing me to work with himself and the other members of the Ford Powertrain Engineering Research and Development Centre at the Essex Engine Plant. I would also like to thank Dr. Iris Xu for her recommendations on my research.

I would also like to thank my colleagues at the Clean Combustion Engine Laboratory for all their time, effort, and suggestions to help improve my understanding of clean combustion research. Thank you for all you have done; Dr. Meiping Wang, Dr. Shui Yu, Dr. Xiao Yu, Dr. Xioye Han, Dr. Tadanori Yanai, Dr. Marko Jeftic, Dr. Prasad Divekar, Dr. Tongyang Gao, Kelvin Xie, Shouvik Dev, Quinyuan Tan, Zhenyi Yang, Chris Aversa, Mark Ives, Zhu Hua, Akshay Ravi, Divyanshu Purohit, and Navjot Sandhu, it has been a pleasure to work with you all.

I would also like to acknowledge Mr. B. Durfy for his assistance in the fabrication of components and equipment for the laboratory and his advice on technical projects.

Finally, I would like acknowledge the following organizations for their funding support: the University of Windsor, Ford Motor Company, the Canada Research Chairs Program, the Canadian Foundation for Innovation, the Ontario Innovation Trust, and the Natural Sciences and Engineering Research Council of Canada.

TABLE OF CONTENTS

LIST OF TABLES

LIST OF FIGURES

LIST OF ABBREVIATIONS

AHRR	Apparent heat release rate	[J/°CA]
CA	Crank angle	[°]
CA5	Crank angle of 5% heat release	[°CA]
CA50	Crank angle of 50% heat release	[°CA]
CA95	Crank angle of 95% heat release	[°CA]
CO	Carbon monoxide	[-]
CO_2	Carbon dioxide	[-]
DI	Direct injection	[-]
dp/dθ	Pressure rise rate	[bar/°CA]
EGR	Exhaust gas recirculation	[-]
EIA	Energy Information Administration	[-]
EPA	Environmental Protection Agency	[-]
GHG	Greenhouse gas	[-]
g/bhp-hr	grams per brake horsepower hour	[g/bhp-hr]
g/hp-hr	grams per horsepower hour	[g/hp-hr]
g/kW-hr	grams per kilowatt hour	[g/kW-hr]
HC	Hydrocarbons	[-]
HCCI	Homogeneous charge compression ignition	[-]
HRR	Heat release rate	[J/°CA]
ICE	Internal combustion engine	[-]
IMEP	Indicated mean effective pressure	[bar]
IVC	Intake valve closing	[°CA]
LTC	Low temperature combustion	[-]
MFB	Mass fraction burned	[%]
NO_x	Nitrogen oxides	[-]
O_2	Oxygen	[-]
PCCI	Premixed charge compression ignition	[-]
p	Cylinder pressure	[bar]
PFI	Port fuel injection	[-]

PM	Particulate matter	[-]
PCCI	Premixed charge compression ignition	[-]
RCCI	Reactivity controlled compression ignition	[-]
TDC	Top dead centre	[-]

CHAPTER 1: INTRODUCTION

1.1 Thesis Outline

The thesis is presented as illustrated in Figure 1-1. The outline of this thesis is as follows, first an introduction explaining the motivation and objective of this work, and summary of the clean combustion strategies to be investigated, and a summary of cycle-to-cycle research to date. Explained in the experimental setup chapter is the configuration of the engine test cell that was used at the clean combustion engine laboratory to collect the data for this thesis, additionally in this section the method of data analysis for determining combustion variation is outlined. Following which the results from the engine tests are presented in Chapter 3 and 4, first diesel only combustion, then ethanol and diesel dual fuel combustion. Finally, the results are summarised and future work is proposed.

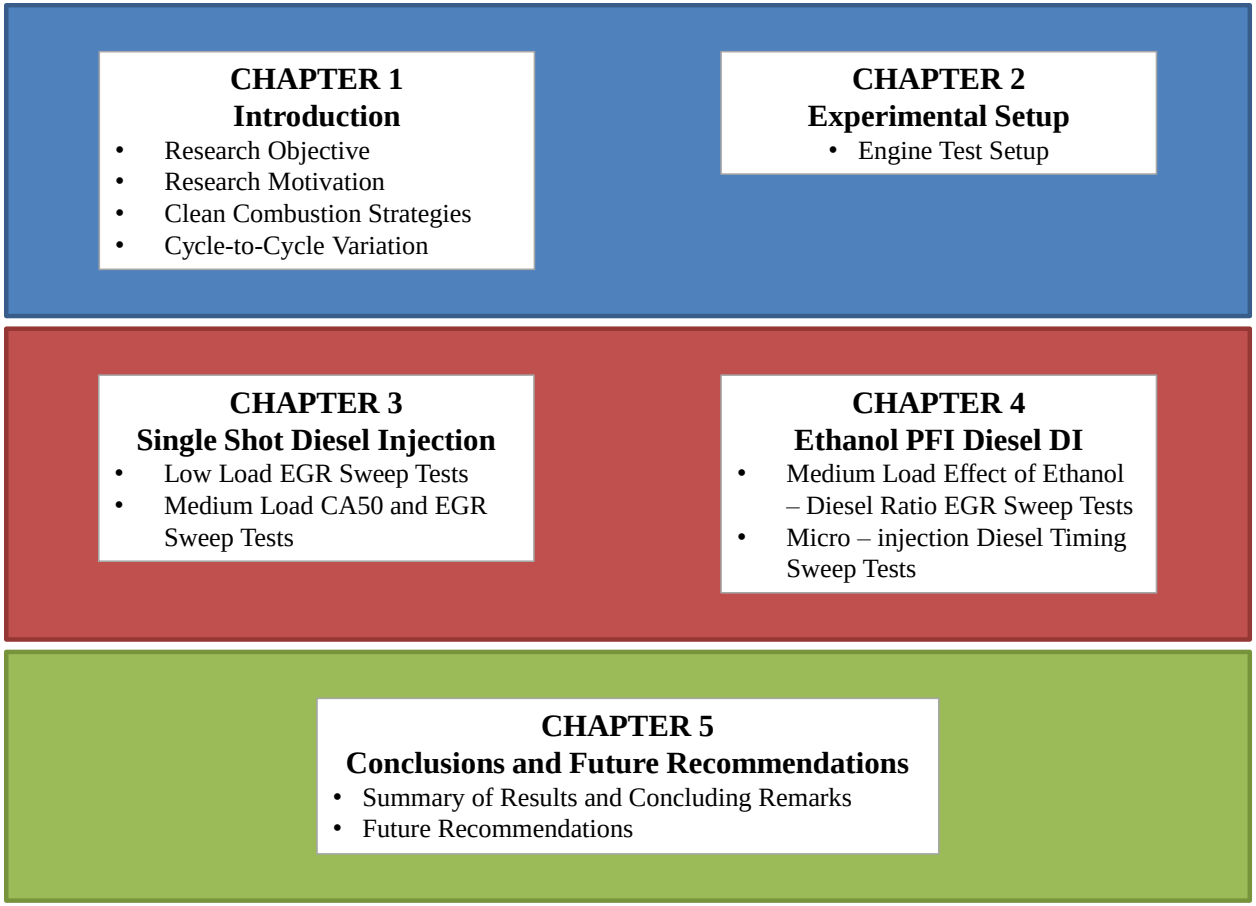

Figure 1-1 Thesis Structure

1.2 Research Objective

The objective of this research was to investigate the cycle-to-cycle variation of two fueling strategies. The first strategy investigated was diesel single shot injection and the second was ethanol port fuel injection (PFI) with diesel direct injection (DI), and the applicability of implementing this dual-fuel strategy from a combustion stability perspective. The tests focused on the effect of exhaust gas recirculation (EGR) and combustion phasing.

1.3 Research Motivation

In the year 2014, of all registered highway vehicles in the United States approximately 4.5% were heavy-duty diesel engines [1]. Shown in Figure 1-2 is the distribution of highway vehicles by type in the US in 2014. The Energy Information Administration (EIA) reported that 92% of heavy-duty vehicles used diesel engines in 2013 [2]. The U.S. Environmental Protection Agency (EPA) reported that medium – heavy-duty vehicles produced 22.5% of the total greenhouse gas emissions (based on carbon dioxide CO_2 equivalent) from the highway transport sector, as shown in Figure 1-3 [3]. The U.S. Department of Transportation reported that 171.0 billion gasoline equivalent gallons were burnt in 2011, of which 39.9 billion gallons were diesel fuel [1].This means that while the total number of heavy duty diesel engines is low relative to gasoline engines, their impact on greenhouse gas emissions and fuel consumption is of major significance.

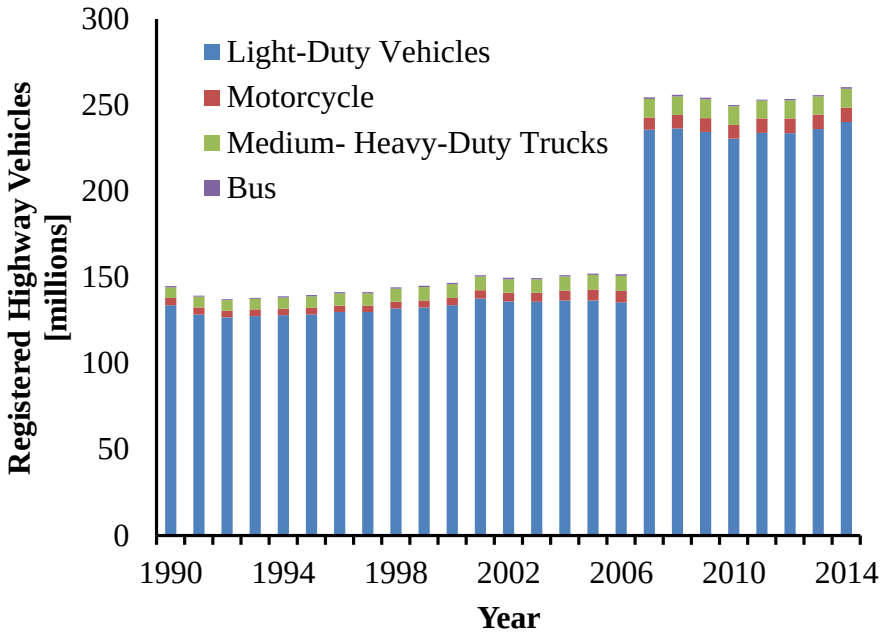

Figure 1-2 Distribution of Registered Highway Vehicles in the U.S. [1]

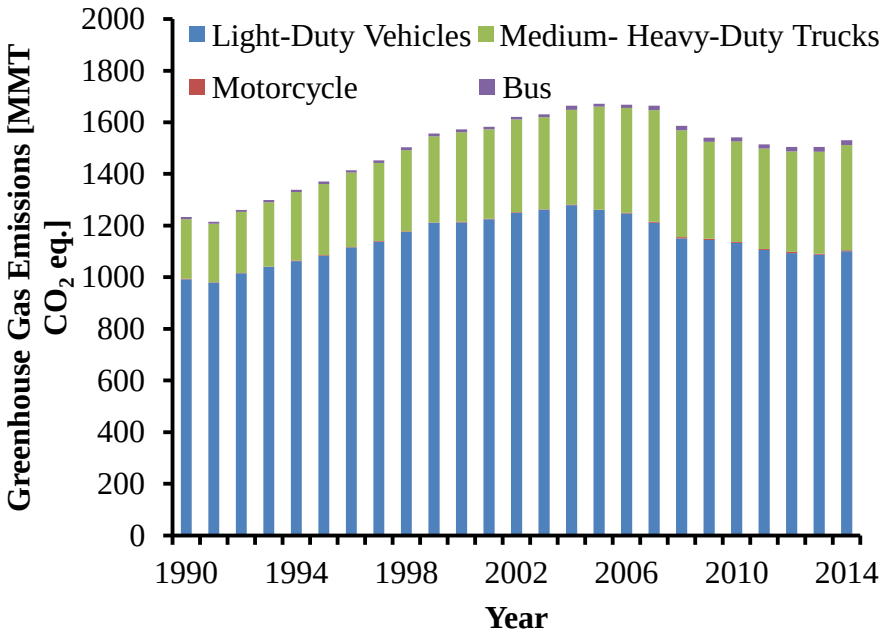

Figure 1-3 Distribution of Greenhouse Gas Emission by Vehicle Type in the U.S. [3]

The primary motivation of this research was to reduce undesirable emissions and improve fuel efficiency, or reduce CO_2 emissions, of diesel engines. This is reflected in government sanctioned emission standards which are becoming increasingly stringent, meaning that a combination of traditional combustion strategies and after-treatment devices must be used in order to meet the new standards. Engine manufacturers have been required to develop new combustion strategies to reduce in-cylinder emissions, primarily oxides of nitrogen (NO_x) and particulate matter (PM). Since 1988, there has been over a 98% reduction in legislated NO_x and PM emission as shown in Figure 1-4 [5]. In 2007, the legislation for NO_x and PM is 0.2 g/bhp·hr and 0.01 g/bhp·hr respectively, additionally in 2015, manufacturers were given the option to certify their engines to the California Low NO_x Standard of 0.1, 0.05, or 0.02g/bhp·hr [5].

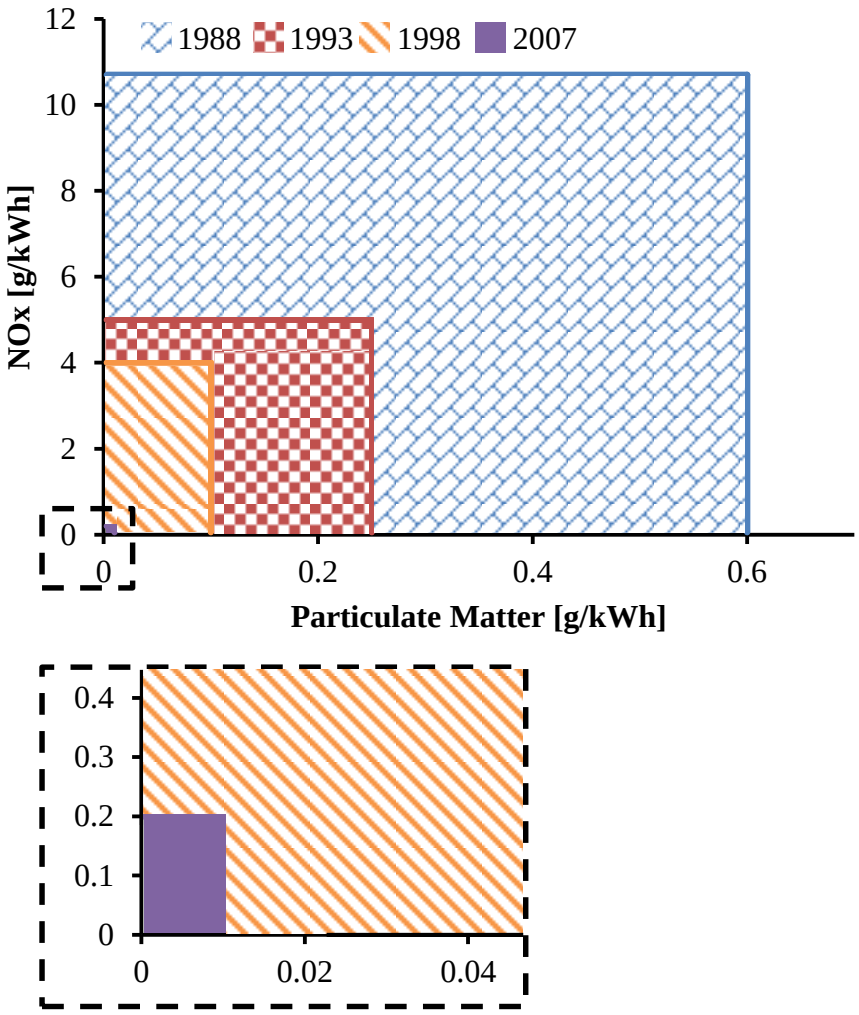

Figure 1-4 EPA Emission Legislation of NO_x and PM [5]

In addition to NO_x and PM restrictions, the EPA will also be implementing carbon dioxide (CO_2) emission standards projected at a 25% reduction by model year 2027 [4]. In order to simultaneously meet the NO_x, PM, and CO_2 emissions, it is necessary to develop clean combustion strategies. With the application of these new combustion strategies there may be an increase in cycle-to-cycle variation, this can cause driveability issues or even misfire if the variation becomes excessive. The combustion stability of diesel and diesel – ethanol dual fuel LTC will be investigated.

1.4 Clean Combustion Strategies

Low temperature combustion (LTC) is a combustion strategy that simultaneously results in ultra-low NO_x and smoke emissions. Ogawa et al. [6] reported that at ultra-high EGR levels smokeless combustion is achievable and the resultant combustion is HCCI-like due to combustion occurring after the conclusion of injection. Akihama et al. [7] presented the potential of smokeless rich diesel combustion through the use of large quantities of EGR, referred to as UNIBUS. Jacobs et al. [8] demonstrated the achievement of LTC through premixed compression ignition (PCI) using high EGR levels and retarded injection timings. The majority of these strategies result in simultaneously low NO_x and soot emissions.

An example of LTC enabled through the use of EGR is shown in Figure 1-5, which represents the trend of NO_x and smoke emissions when intake oxygen was reduced. With the application of EGR there was a reduction in NO_x emissions. The initial increase in smoke emissions when the intake oxygen concentration was reduced is referred to as slope one. Slope two is the name given to the simultaneous reduction of NO_x and smoke emissions once a sufficiently low intake oxygen concentration was reached. However, this comes at the expense of reduced combustion efficiency, indicated by an increase in CO and THC emissions.

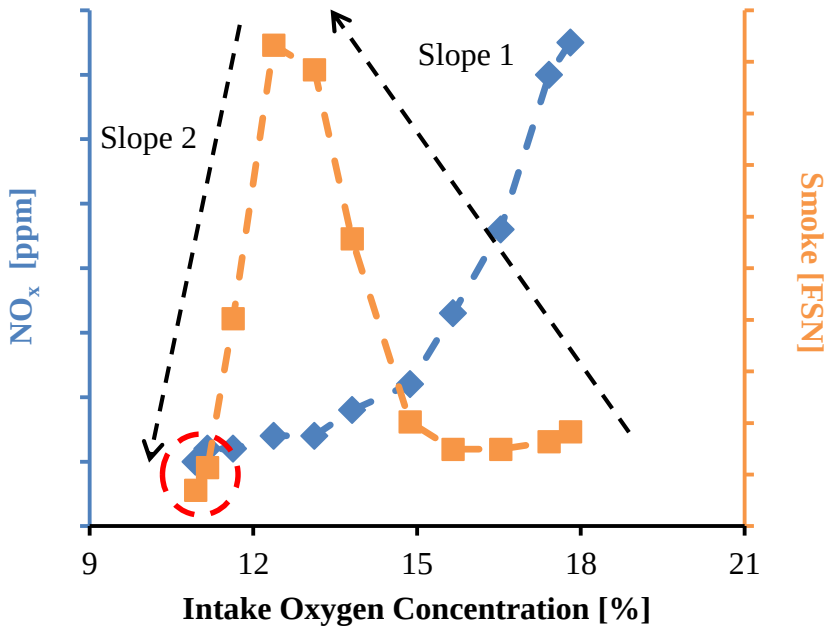

Figure 1-5 NO_x Soot Trade off with Application of EGR

Reitz [9] discussed the research status of advanced internal combustion engines and their advantages over early LTC strategies. The use of reactivity controlled compression ignition (RCCI) can result in improved fuel efficiency and a reduced cost as there is reduced requirement on after-treatment systems, and is suggested as the method of future development.

RCCI can be achieved through the use of two fuels, one low reactivity fuel and one high reactivity fuel, such as ethanol and diesel. The advantage of this strategy is that the low reactivity fuel creates a near homogenous mixture with air, this results in low soot production from combustion, as well as a lower peak cylinder temperature so NO_x production is mitigated. Han et al. [10] showed the ignition of ethanol with a single diesel injection with diesel contributing approximately 20% of the load. Asad et al. [11] used single and double diesel injections to ignite a PFI ethanol – air mixture, it was found that

in the double injection case, the first injection increased the reactivity of the mixture while the second injection provided the ignition energy. Gao et al. [12] investigated the influence of EGR on a range of diesel – ethanol ratios, it was found that with increasing ethanol content, smoke emissions were reduced, and that it was possible to ignite a ratio of 95% ethanol 5% diesel with a single injection. The use of such a low diesel – ethanol ratio could allow for ethanol to be used as the primary fuel source and diesel fuel to only be used as an ignition source.

The LTC strategies used in this research were single shot diesel injection with EGR and RCCI with ethanol PFI and diesel DI in combination with EGR.

1.5 Cycle-to-Cycle Variation in Compression Ignition Engines

There are three commonly used methods for determining cycle-to-cycle variation in engines; in-cylinder pressure, flame, and emission derived parameters. In order to use each of these methods specialist equipment is required. Typically emission derived variations require fast sampling and analysis capabilities of exhaust species, while in order to characterize the flame parameters optical access is typically required. The most common method to determine cyclic variations is to derive them from in-cylinder pressure measurements, this requires measurement of the cylinder pressure in the crank angle domain. In this research it was decided to use in-cylinder pressure derived parameters in order to determine cycle-to-cycle variation. Some of the parameters used in the literature to investigate cyclic variation are indicated mean effective pressure (IMEP), maximum in-cylinder pressure (p_{max}), crank angle of maximum in-cylinder pressure (CA p_{max}), $dp/d\theta_{max}$, CA $dp/d\theta_{max}$, and the crank angle of 50% heat release (CA50).

Kyrtatos et al. [14] investigated the effect of ignition delay on in-cylinder pressure oscillations and cycle-to-cycle variation in a diesel engine, they reported that increasing the ignition delay resulted in greater cyclic variation. Maurya et al. [15] looked at the effect of intake temperature and air-fuel ratio on HCCI combustion of ethanol. The COV_{pmax} increased when the excess air ratio, lambda (λ), was decreased or when the intake temperature was increased for a given air-fuel ratio. Koizumi et al. [16] studied the cycle-to-cycle variation of a two-stroke diesel engine with mechanical fuel injection, and found that the variation in fuel injection quantity was coupled to the cyclic variations of IMEP, however, the variation of p_{max} and IMEP were largely independent. Kyrtatos et al. [17] investigated the cycle-to-cycle of a single-cylinder diesel engine operating in the low temperature regime with a single diesel fuel injection. It was determined that long ignition conditions resulted in a greater portion of combustion being premixed type combustion, which, resulted in an increase in cyclic variations. Sen et al. [18] studied the cycle-to-cycle variation of mean indicated pressure of a diesel engine at different engine speeds, it was found that at certain speeds the variation was more periodic, while at others it was more intermittent. It was also stated that the decreased time for mixing results in a more ordered combustion process as the ignition timing was determined primarily by the geometrical position of the piston. Wang et al. [19] investigated the cyclic variation of a diesel engine operating using port fuel injected dimethyl ether and direct injected diesel. It was reported that increasing the quantity of dimethyl ether while maintaining the same load resulted in an increase in the variation of p_{max}, $dp/d\theta_{max}$, and IMEP. Ali et al. [20] found that when diethyl ether was added to a 30% biodiesel 70% petroleum diesel blend the cycle-to-cycle variations increased. From these findings it was expected that cycle-to-cycle variations

would increase as the premixed portion of combustion was increased, either through the use of EGR or with the use of port fuel injected ethanol.

CHAPTER 2: EXPERIMENTAL SETUP

The engine test bed used in this thesis was located in the Clean Combustion Engine Laboratory at the University of Windsor. The engine used for this study was an inline 4-cylinder 2.0 L Ford Puma Doratorque converted to a 1 research – 3 motoring cylinder configuration by the author's colleagues, for full details of the conversion please refer to [21]. The physical specifications of the engine are given in Table 2-1.

Table 2-1 Engine Geometric Specifications

Bore [mm]	86
Stroke [mm]	86
Connecting Rod Length [mm]	144
Compression Ratio [-]	18.2:1
Displacement Volume [L]	1.999

The test cell had the capability to independently control the intake pressure, exhaust gas recirculation, injection pressure, injection duration, and injection timing. A schematic of the test cell is shown in Figure 2-1. The boost pressure was simulated using an oil-free dry air compressor, the intake and exhaust surge tanks were used to mitigate pressure wave action. The exhaust gas recirculation was controlled with a combination of an EGR valve and an exhaust backpressure valve. The intake pressure and EGR were controlled using PC based LabVIEW programs developed in house. Additionally, the temperatures and air flow were monitored and recorded. The high pressure injection in each cylinder was controlled with a combination of injector drivers, National Instruments Real Time – Field

Programmable Gate Array hardware, and an in-house developed LabVIEW program. Port fuel injection was possible for the research cylinder using a similar configuration. Exhaust emissions were sampled downstream of the exhaust surge tank using a bank of California Analytical Instruments (CAI) emission analyzers and an AVL smoke meter, details are given in Table 2-2. The CAI emission analyzers gave volumetric concentration measurements of the gaseous species, as such all gaseous emission results are reported on a volumetric basis. The AVL smoke meter measured the smoke emissions in Filter Smoke Number (FSN), as defined according to ISO 10054.

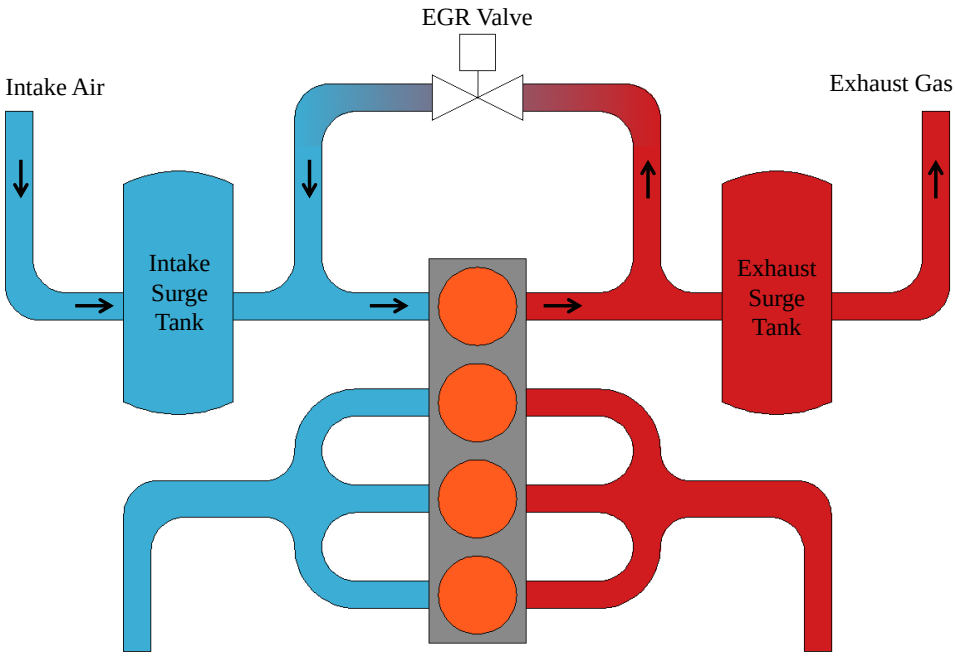

Figure 2-1 Schematic of Ford PUMA Engine Configuration

Table 2-2 Emission Analysers

Analyzer Model	Measured Emission	Measurement Range
CAI 602P	O_2	0 – 21 [%]
CAI 300M HFID	THX	0 – 20000 [ppm]
CAI 200/300 NDIR	CO & CO_2	0 – 5000 [ppm] & 0 – 40 [%]
CAI 600 HCLD	NO & NO_2	0 – 3000 [ppm]
AVL Model 415S	Smoke	0 – 10 [FSN]

The engine rotation was measured with a Gurley optical encoder capable of crank angle resolution up to 0.05° CA, this was coupled with the pressure measurement to record pressure data in the crank angle domain to easily calculate volumetric derived parameters such as IMEP. For continuous measurement the pressure data was reordered at 1 °CA and for each testing point 200 consecutive cycles were recorded at 0.1 °CA

The engine was also able to run on different fuels and fueling strategies, the fuels available for use are diesel and ethanol, the fuel specifications are given in Table 2-3.

Table 2-3 Fuel Properties [22, 23]

Fuel Properties	Diesel	Ethanol
Octane Number	25	110 - 115
Cetane Number	46.5	8 – 11
Lower Heating Value [MJ/kg]	43.1	27
Oxygen $Content_{mass}$ [%]	0	34.8
Boiling Temperature [°C]	341	78
Latent Heat of Vaporization [kJ/kg]	316.6	728.2
Density [kg/m^3]	846	780
Kinematic Viscosity [cSt]	>3	1.52

.

CHAPTER 3: DIESEL SINGLE SHOT COMBUSTION

This chapter is presented in three sections. First the effect of EGR on low load single shot diesel combustion is investigated, followed by the effect of EGR and combustion phasing on 10 bar single shot diesel combustion. Then a summary of the chapter will be given.

3.1 Effect of EGR on Low Load Single Shot Diesel Combustion

Reported in this section is the effect of EGR on low load diesel single shot combustion at two different engine speeds, 1800 rpm and 2400 rpm. The test matrix is shown in Table 3-1. The two tests are identified by their initial indicated load.

Table 3-1 Test Matrix for Effect of EGR at Low Load

	3.5 bar IMEP	6.1 bar IMEP
Inj. Timing [°CA]	357.7 – 352.5	351.0 – 349.0
Inj. Duration [μs]	440	540
Inj. Pressure [bar]	900	900
T_{Intake} [°C]	35 - 58	39 - 58
p_{Intake} [bar_{gauge}]	0.5	0.5
Engine Speed [rpm]	1800	2400
Intake Oxygen [%]	17.7 – 10.5	18.8 – 13.3
IMEP [bar]	3.5	6.1
CA50 [°CA]	369.0 – 368.7	368.5 – 368.1

Some fluctuations in IMEP and CA50 were observed with decreasing intake oxygen, the injection timing was adjusted in order to minimise the change in CA50.

Shown in Figure 3-1 is the effect of EGR on the NO_x emissions for the two data sets. As has been reported in literature [6 - 8, 24] with increasing EGR there was a decrease in NO_x emissions. Eventually the NO_x emissions are reduced to less than 40 ppm for both load levels. Less NO_x was produced at a lower engine load, as the peak temperature was also lower with leaner mixtures.

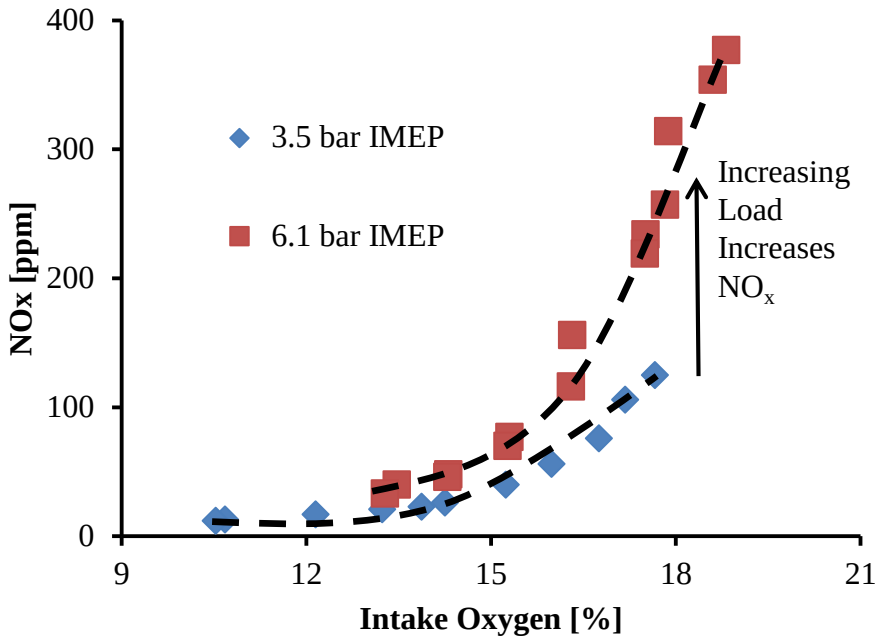

Figure 3-1 Effect of EGR on Low Load NO_x Emissions

Shown in Figure 3-2 is the effect of EGR on PM emissions, here it can be seen that there was an increase in smoke emissions with decreasing intake oxygen. In the 3.5 bar IMEP test at approximately 12% intake oxygen the smoke emissions begin to reduce again, referred to as slope two, resulting in simultaneously low NO_x and PM, however LTC is not completely achieved, further EGR would need to be applied to reach the "ultra-low" threshold. However for the 6.1 bar IMEP as the smoke emissions were over 4.0 FSN which is equivalent to approximately 0.3 g/hp·hr, 15 times the PM legislated limit, so further EGR was not applied.

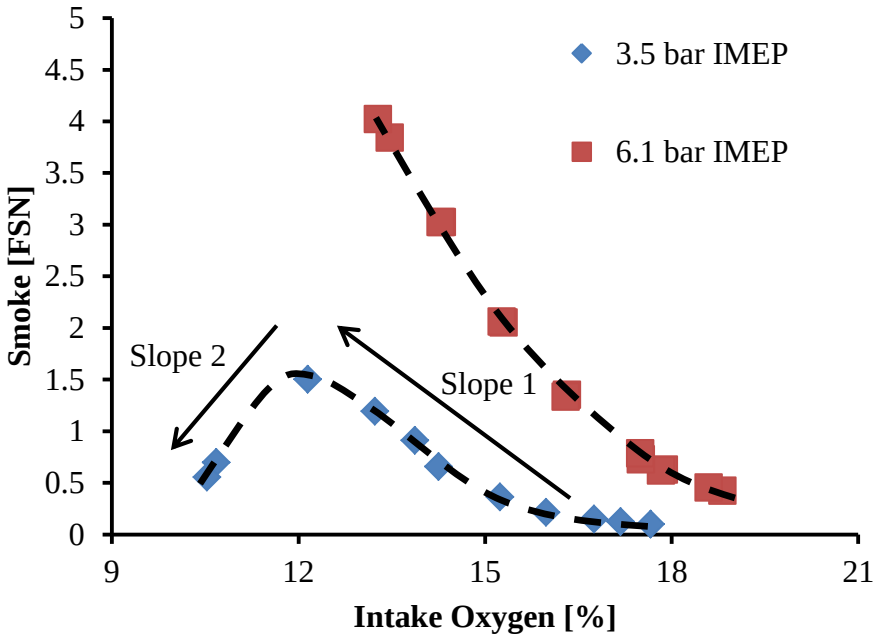

Figure 3-2 Effect of EGR on Low Load PM Emissions

The injection timing was adjusted in order to minimise the loss of IMEP caused by increasing EGR, which is shown in Figure 3-3.

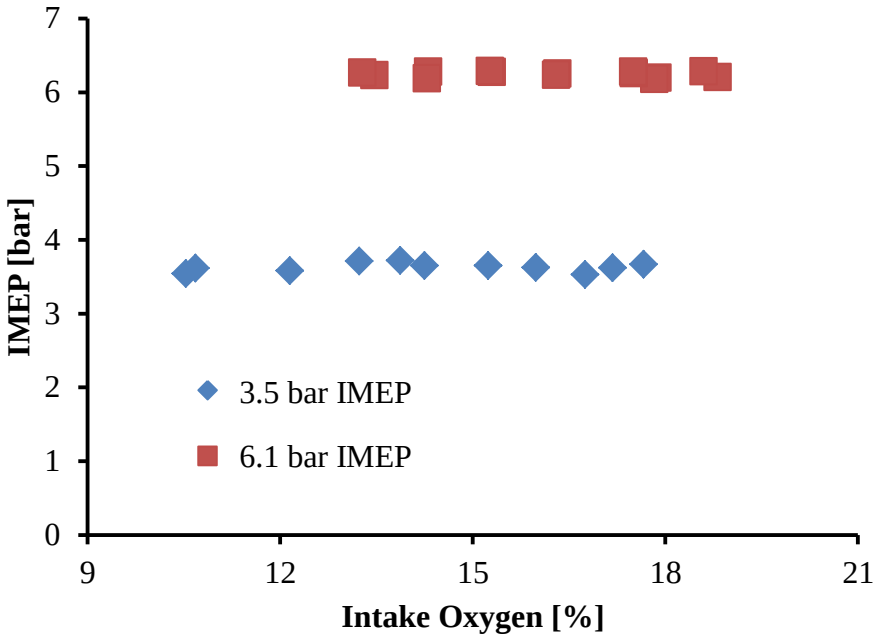

Figure 3-3 Effect of EGR on Engine Load at Low Load

The effect of intake oxygen on ignition delay is shown in Figure 3-4, with decreasing intake oxygen there was an increase in ignition delay, which allowed more time for mixing.

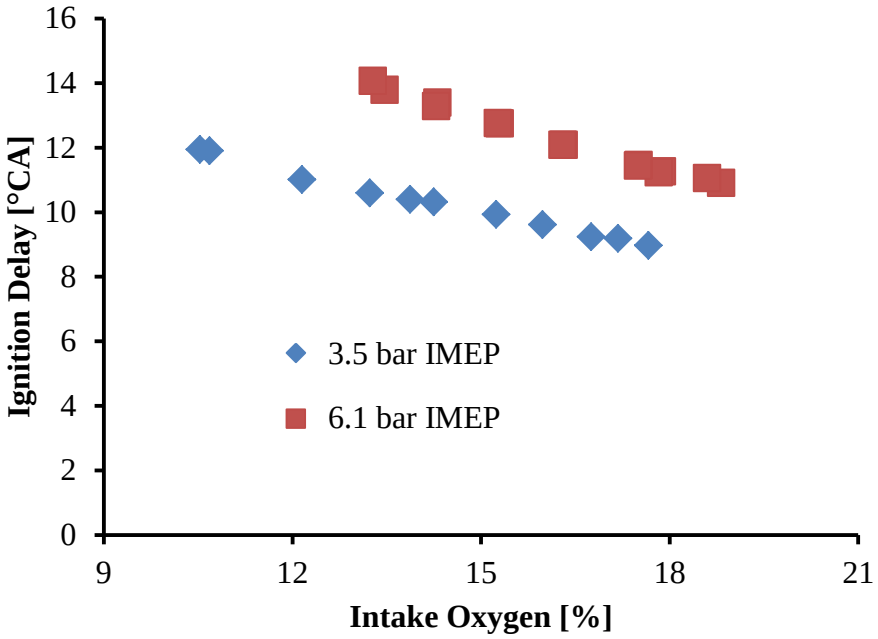

Figure 3-4 Effect of EGR on Ignition Delay at Low Load

The effect of intake oxygen on CA50 is shown in Figure 3-5, as previously mentioned the injection timing is adjusted to compensate for the effect of EGR on the phasing of CA50 so there is minimal change in CA50 with decreasing intake oxygen concentration.

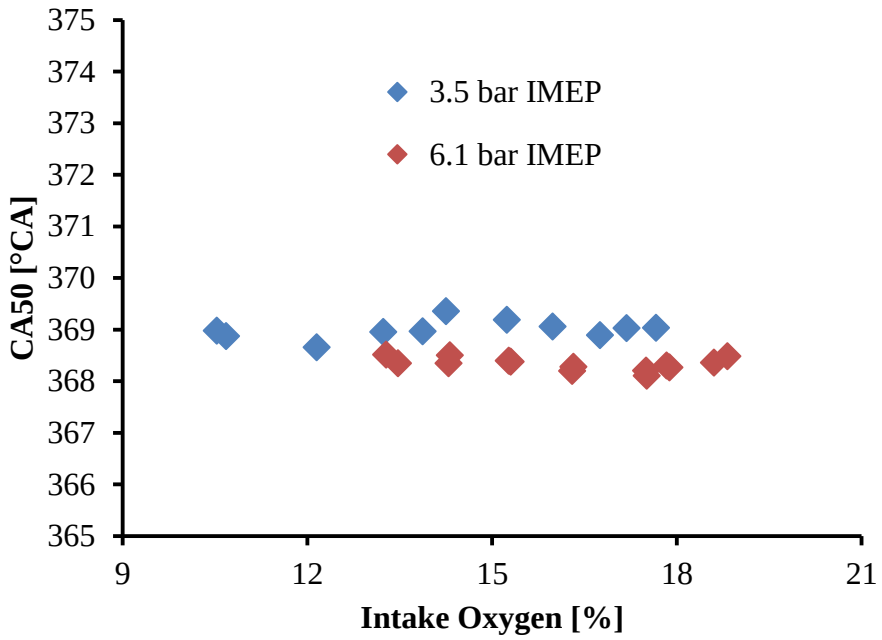

Figure 3-5 Effect of Intake Oxygen on CA50 At Low Load

The combustion stability will be presented using the COV_{IMEP} and the standard deviation of CA50. The COV_{IMEP} is used to describe how reliable power production is while the standard deviation of CA50 describes how consistent the combustion phasing is. Excessive variation in combustion stability can result in misfire or excessive peak pressure which can result in high quantities of undesirable emissions, driveability issues, or potential damage to the engine [13, 15, 17]. The COV_{IMEP} changed minimally when the intake oxygen concentration was above 13%, however when reduced below 13% there was an exponential increase in the COV_{IMEP} which is shown in Figure 3-6.

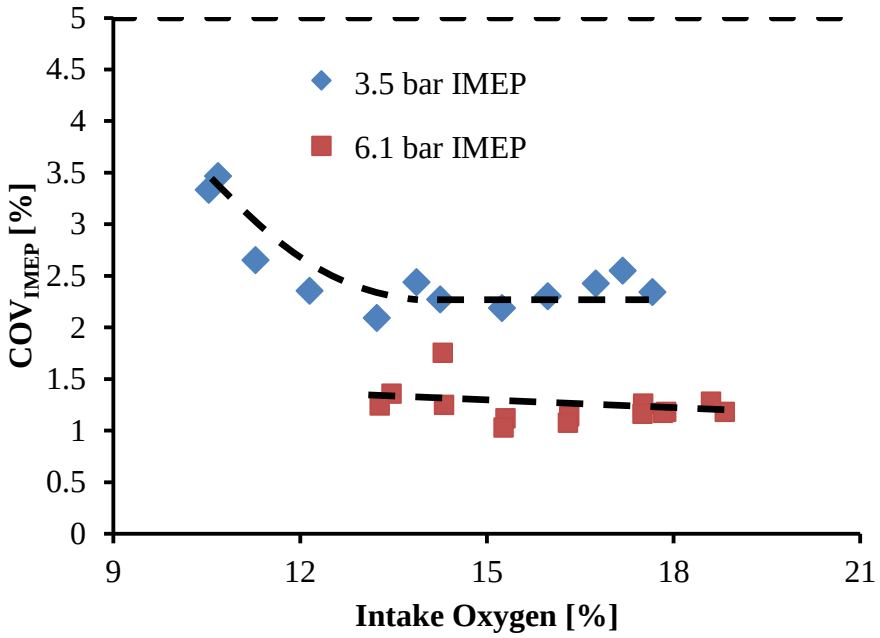

Figure 3-6 Effect of Intake Oxygen on COV_{IMEP} at Low Load

The effect of EGR on the standard deviation of CA50 is shown in Figure 3-7. For intake oxygen concentrations from ambient to approximately 13% there was minimal effect, however, at intake oxygen concentrations less than 13% there was an increase in the standard deviation of CA50. The increase in the combustion instability could be caused by the reduced reactivity of the in-cylinder charge. The reduced reactivity of the cylinder charges could sufficiently shift the combustion initiation away from a purely physical mixing process to a combined mixing and chemical kinetic process which is more sensitive to the background temperature and chemical species.

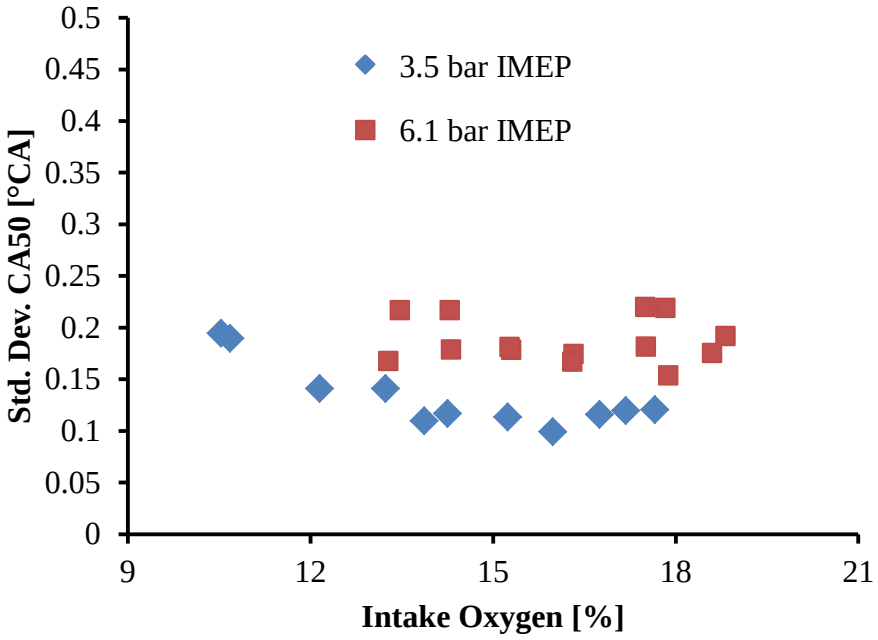

Figure 3-7 Effect of Intake Oxygen on the Standard Deviation of CA50 at Low Load

Shown in Figure 3-8 and Figure 3-9 are the 200 consecutive cycle pressure and heat release rate traces for the highest and lowest intake oxygen for the 3.5 bar IMEP test. Illustrated in Figure 3-8 are the pressure and heat release rate traces for 200 consecutive cycles, as well as the average pressure and heat release trace (shown with a black dashed line) for the 3.5 bar IMEP test at 17.7% intake oxygen. This is representative of a HTC mode due to the high HRR rate and short combustion duration. The mean, minimum, maximum, and variation of the maximum cylinder pressure, IMEP, and CA50 are shown in Table 3-2.

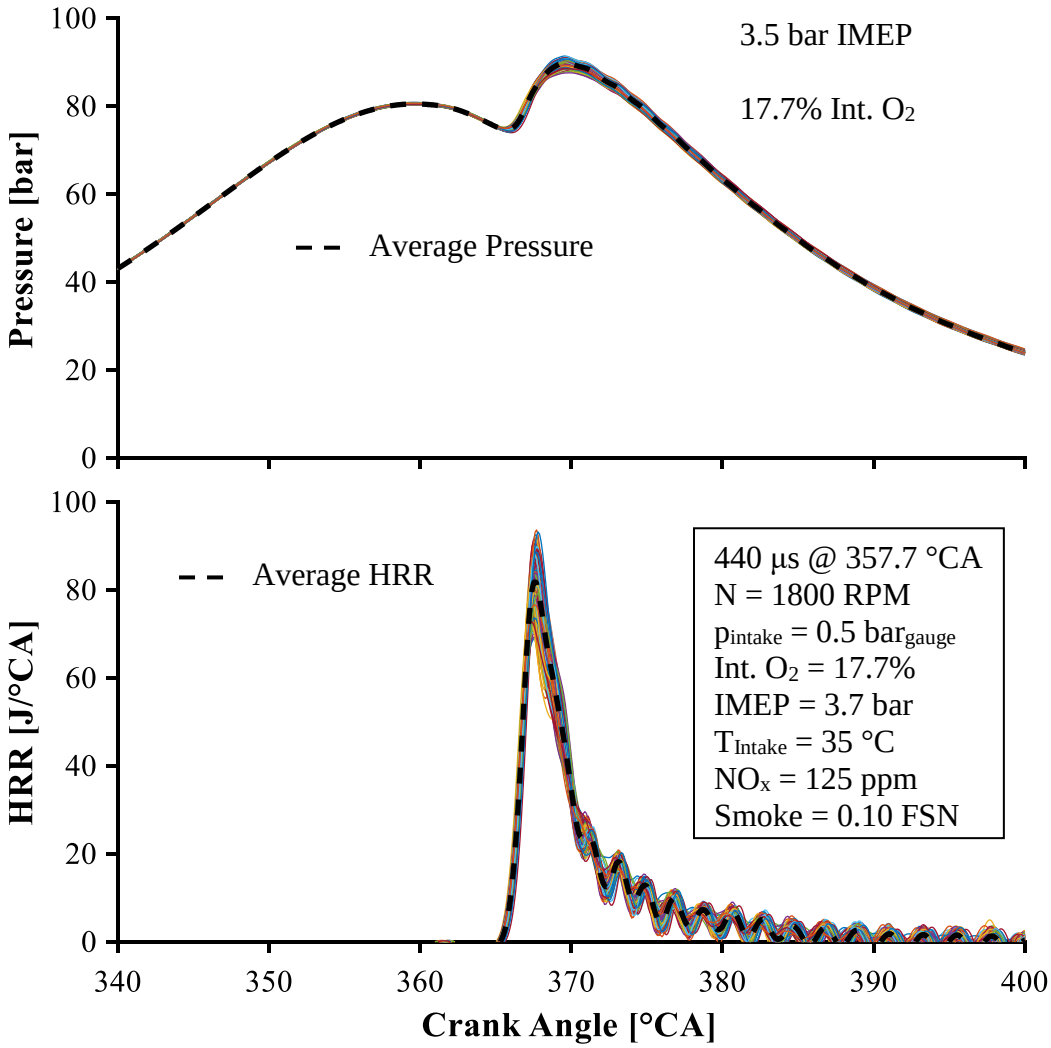

Figure 3-8 200 Cycle Pressure and HRR Trace of 3.5 bar IMEP 17.7% Intake Oxygen

Table 3-2 Combustion Parameters of 3.5 bar IMEP at Low EGR 200 Cycle Data

Parameter	Mean	Minimum	Maximum	Variation
p_{max}	89.9 bar	87.6 bar	91.4 bar	0.8%
IMEP	3.7 bar	3.5 bar	3.9 bar	2.3%
CA50	369.0 °CA	368.8 °CA	369.5 °CA	0.1 °CA

Shown in Figure 3-9 are the 200 consecutive cycles of pressure and heat release traces for the lowest intake oxygen condition, 10.5%, which resulted in low NO_x and relatively low PM emissions. The mean, minimum, maximum, and variation of the maximum cylinder pressure, IMEP, and CA50 are shown in Table 3-3. With the reduction of intake oxygen from 17.7% to 10.5% there is a reduction in the mean values of p_{max} and IMEP of 3.3 and 0.2 bar respectively. There is also an increase in the variation of p_{max}, IMEP, and CA50 with increase EGR. The reduction of intake oxygen concentration to 10.5% reduced the peak HRR and increased the combustion duration, which resulted in a lower peak cylinder temperature and therefore, less NO_x emissions were produced.

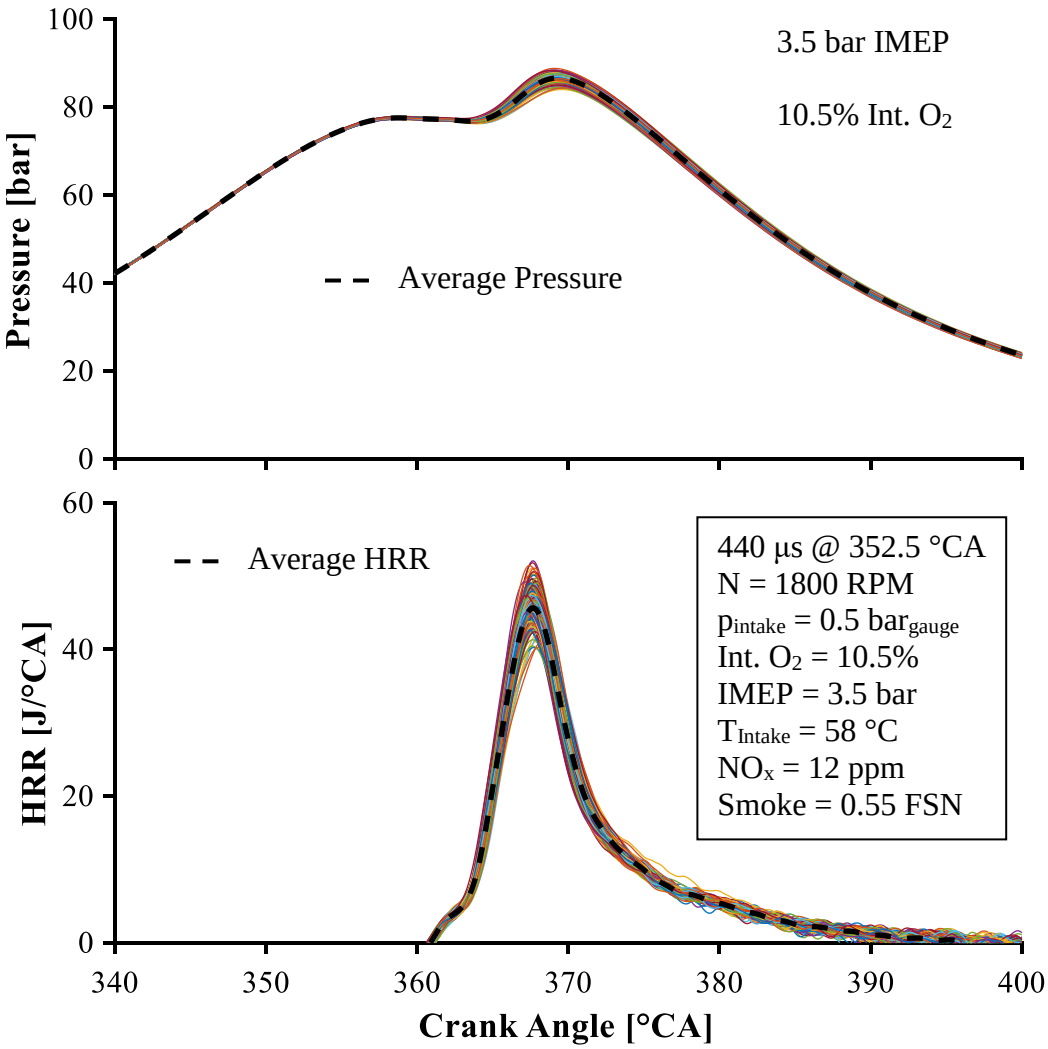

Figure 3-9 200 Cycle Pressure Trace of 3.5 bar IMEP 10.5% Intake Oxygen

Table 3-3 Combustion Parameters of 3.5 bar IMEP at High EGR 200 Cycle Data

Parameter	Mean	Minimum	Maximum	Variation
p_{max}	86.6 bar	84.0 bar	88.8 bar	1.1%
IMEP	3.5 bar	3.2 bar	3.9 bar	3.3%
CA50	369.0 °CA	368.5 °CA	369.7 °CA	0.2 °CA

Presented in this section was the effect of EGR on two low load conditions, 3.5 and 6.1 bar IMEP. While neither condition reached LTC the 3.5 bar test did reach slope 2, the simultaneous reduction of NO_x and soot. Eventually reaching 12 ppm and 0.55 FSN NO_x and PM emission respectively at 10.5% intake oxygen. The cyclic variation of IMEP was higher for the lower load condition for all intake oxygen concentrations which agreed with the literature [6 – 8]. However, the variation of CA50 was greater for the high load test conditions for the same intake oxygen concentration, this could be related to different periodic oscillations at different engines speeds as found by Sen et al. [18]. For the 3.5 bar IMEP test at approximately 12% intake oxygen, there was an increase in the COV_{IMEP} from 2.1% to 3.5% with decreasing intake oxygen. A possible reason for this was that with the reduced reactivity at intake oxygen concentrations lower than 12% the ignition was more sensitive to changes in the background environment, both physical and chemical properties, such as changes in temperature, pressure, and species concentration.

3.2 Effect of EGR and CA50 at 10 bar IMEP

The investigation of the influence of EGR and combustion phasing on medium load, 10 bar IMEP, single shot diesel combustion is presented in this chapter.

The test conditions are shown in Table 3-4. The injection pressure, intake pressure, and engine speed were kept constant in each case. Injection timing was adjusted with the application of EGR in order to maintain an approximately constant CA50.

Table 3-4 10 bar Single Shot Diesel Test Conditions

	Case 1	Case 2	Case 3
Inj. Timing [°CA]	356.7 – 352.1	359.8 – 356.3	368.7 – 362.9
Inj. Duration [μs]	525	525	575
Inj. Pressure [bar]	1500	1500	1500
T_{Intake} [°C]	24 – 47	37 – 51	39 – 53
p_{Intake} [bar]	1.0	1.0	1.0
Engine Speed [rpm]	1500	1500	1500
Intake Oxygen [%]	17.8 – 10.6	18.5 – 11.7	17.8 – 10.9
IMEP [bar]	10.0 – 9.0	10.0 – 9.4	9.8 – 8.1
CA50	366.9 – 365.6	370.0 – 368.9	380.7 – 380.1

The cases are distinguished by their CA50, or combustion phasing, case 1 is represented in the proceeding figures as CA50 366, case 2 is represented in the proceeding figures as CA50 369, and case 3 is represented in the proceeding figures as CA50 380.

Not all cases were able to reach LTC operating conditions, which were characterized by simultaneous ultra-low NO_x and PM emissions, which can be seen in Figure 3-10 and Figure 3-11.

The effect of intake oxygen on NO_x emissions is illustrated in Figure 3-10. With decreasing intake oxygen there was a reduction in NO_x emissions, resulting in less than 20 ppm for all cases. Figure 3-10 also shows that the later combustion phasing resulted in lower NO_x emissions at the highest intake oxygen conditions, the CA50 380 case produced 73% less NO_x than the CA50 366 case, on ppm basis.

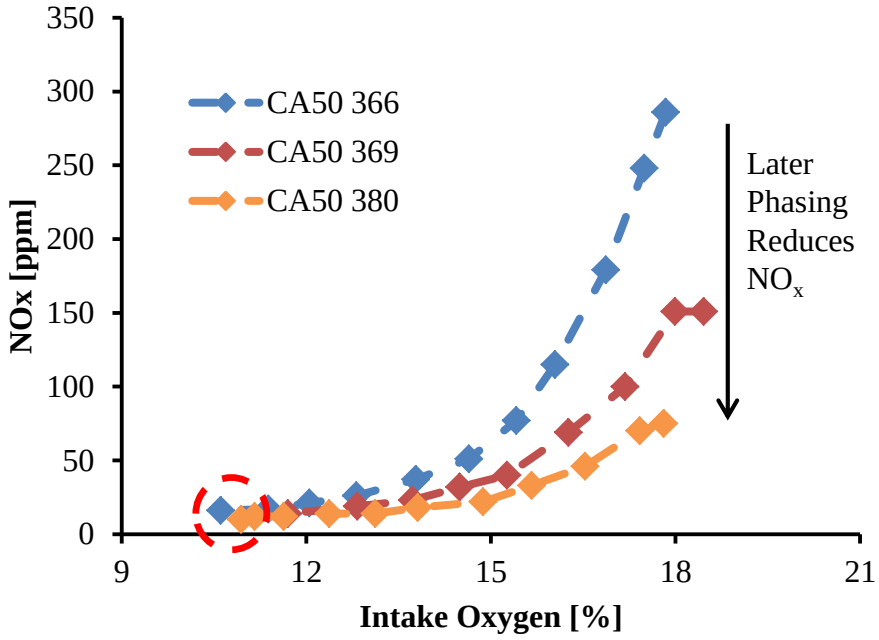

Figure 3-10 Influence of Intake Oxygen on NO_x Emissions at Medium Load

The effect of EGR on smoke emissions is shown in Figure 3-11. With increasing EGR ratio there was an initial increase in smoke emissions for all tests. However for the CA50 380 cases a peak smoke value was reached at approximately 12.5% intake oxygen, after which smoke emissions rapidly reduced until they were less than 0.2 FSN. By comparison the smoke emissions of the CA50 366 and 369 °CA tests increased with decreasing intake oxygen to approximately 5 FSN.

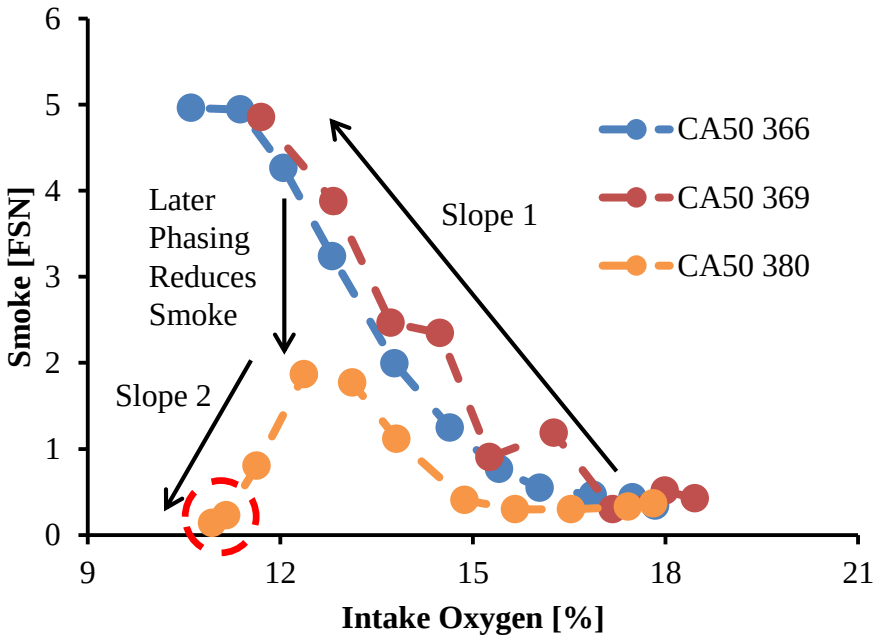

Figure 3-11 Influence of Intake Oxygen on PM Emissions at Medium Load

With the simultaneous reduction of NO_x and PM there was a significant increase in the CO and HC emissions, or combustion inefficiency. The increase in CO and THC emissions was also exhibited by a reduction in engine load, this is shown in Figure 3-12, with decreasing intake oxygen there was a decrease in IMEP for all cases.

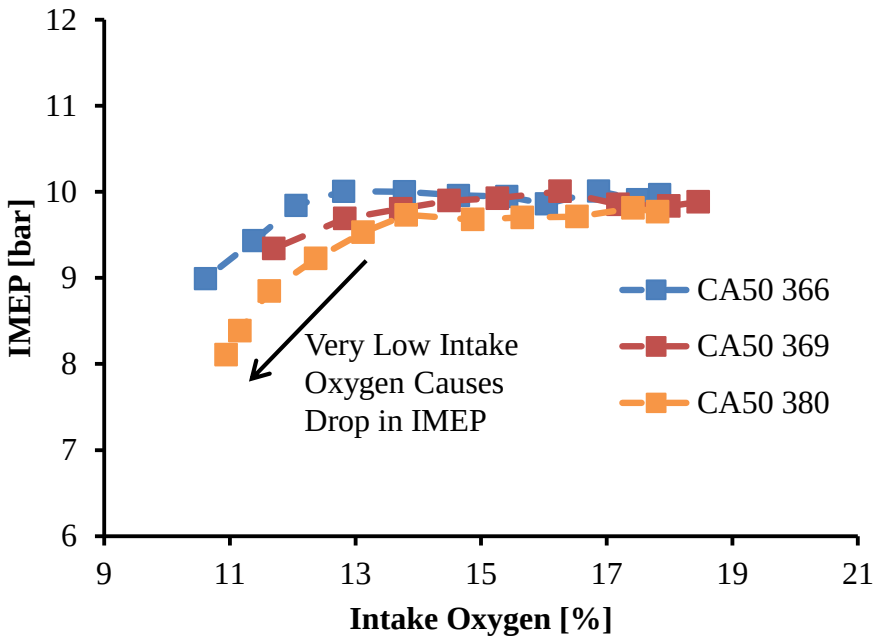

Figure 3-12 Influence of Intake Oxygen on IMEP at Medium Load

Shown in Figure 3-13 and Figure 3-14 is the effect of intake oxygen on CO and THC emissions for the three combustion phasing timings at 10 bar IMEP for diesel single shot combustion. For both THC and CO emissions there was minimal change with increasing EGR until the intake oxygen was below 15%, at which point there was an exponential increase with increasing EGR. For a given intake oxygen concentration the CO and THC emissions were highest for the CA50 380 case due to the very late combustion phasing resulting in incomplete combustion. All test conditions resulted in the CO concentrations exceeding 5000 ppm which was beyond the CO emission analyser's measurement range. The CA50 380 °CA saturated the analyser at the highest intake oxygen level. The increase in CO and THC emissions was reflected in the reduction of IMEP. For the low temperature combustion conditions, CA50 380 °CA at 11.16% and 10.94% intake oxygen concentration, the soot and NO_x emissions were ultra-low , < 0.227 FSN and < 20 ppm respectively. However this was at the expense of high CO and THC emissions in excess of 5000 ppm and 850 ppm respectively. In order to obtain ultra-low NO_x and PM for a single diesel injection at 10 bar IMEP it was necessary to sacrifice combustion and fuel efficiency.

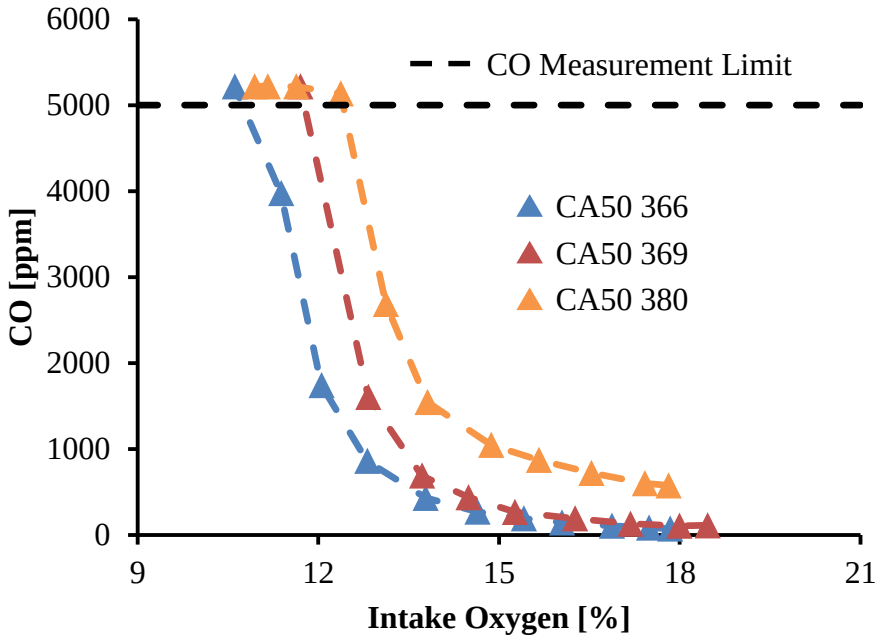

Figure 3-13 Effect of Intake Oxygen on CO Emissions at Medium Load

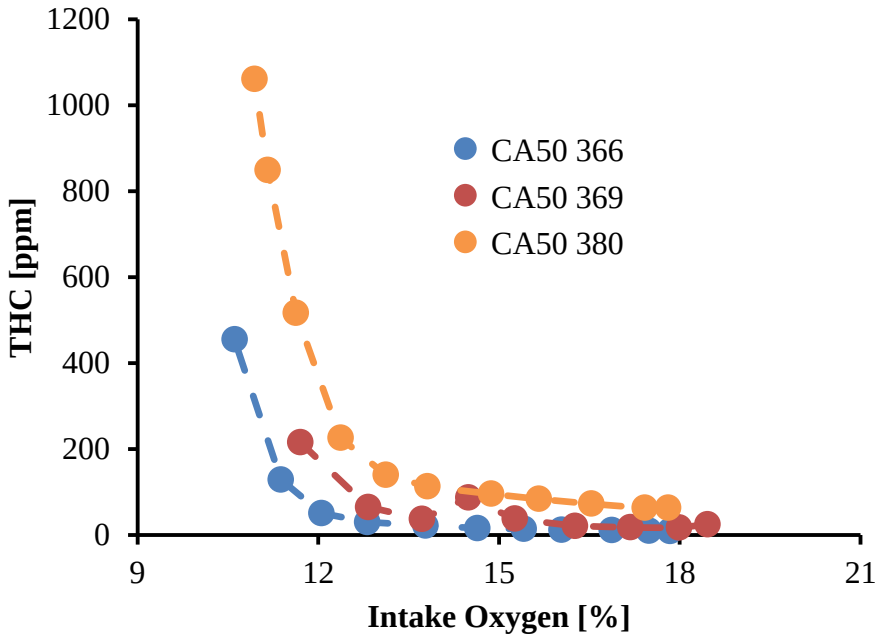

Figure 3-14 Effect of Intake Oxygen on THC Emissions at Medium Load

The COV_{IMEP} for all three cases is displayed in Figure 3-15 as well as the 5% limit. The COV_{IMEP} was below the specified limit, but it was greater than the COV_{IMEP} observed for 6.1 bar case shown in Figure 3-6. However, there was no apparent trend between the COV_{IMEP} and the intake oxygen concentration. The CA50 366 and 369 tests, had a slight reduction in the COV_{IMEP} with reducing intake oxygen concentration. While the latest combustion phasing case had minimal change with intake oxygen concentration. This was different from the low load tests, Figure 3-6, where below 13% intake oxygen there was a noticeable increase in combustion instability.

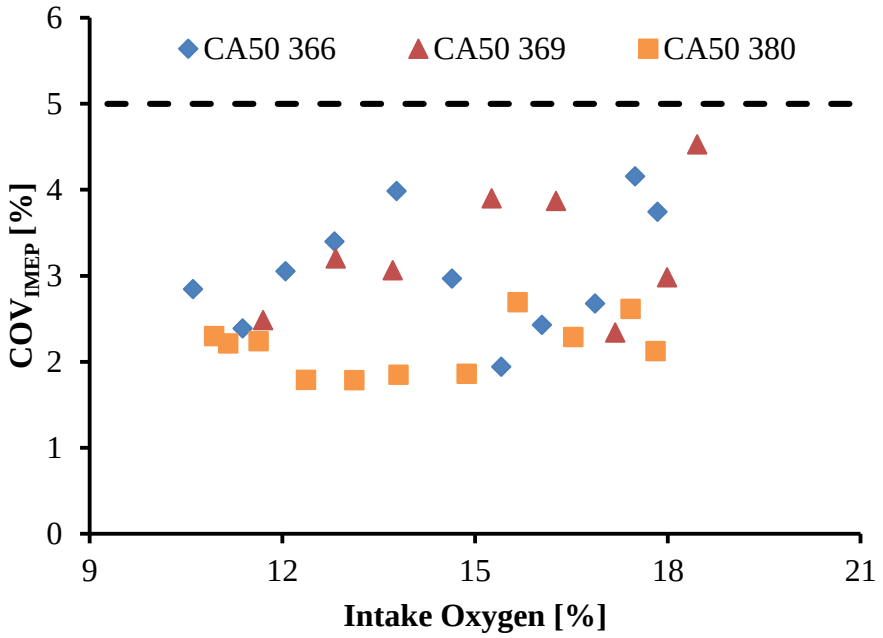

Figure 3-15 Influence of Intake Oxygen on COV of IMEP at Medium Load

The influence of intake oxygen on the standard deviation of CA50 is shown in Figure 3-16. All of the cases showed a similar trend, an increase in the standard deviation of CA50 with reducing oxygen. The effect was a gradual linear increase in the traditional combustion phasing cases, for optimal efficiency the CA50 should occur between 360 and 370 °CA. Whereas for the CA50 380 °CA test the linear trend was considerably steeper almost doubling when the intake oxygen was reduced from 17.8% to 10.9%. The CA50 380 °CA had a greater variation of CA50 for all intake oxygen concentrations. While the variation of engine load was more stable at the CA50 380 °CA condition the variation of combustion phasing was greater, further analysis should be done to determine at which point, if any, the variation of CA50 becomes more influential on combustion stability than the COV_{IMEP}.

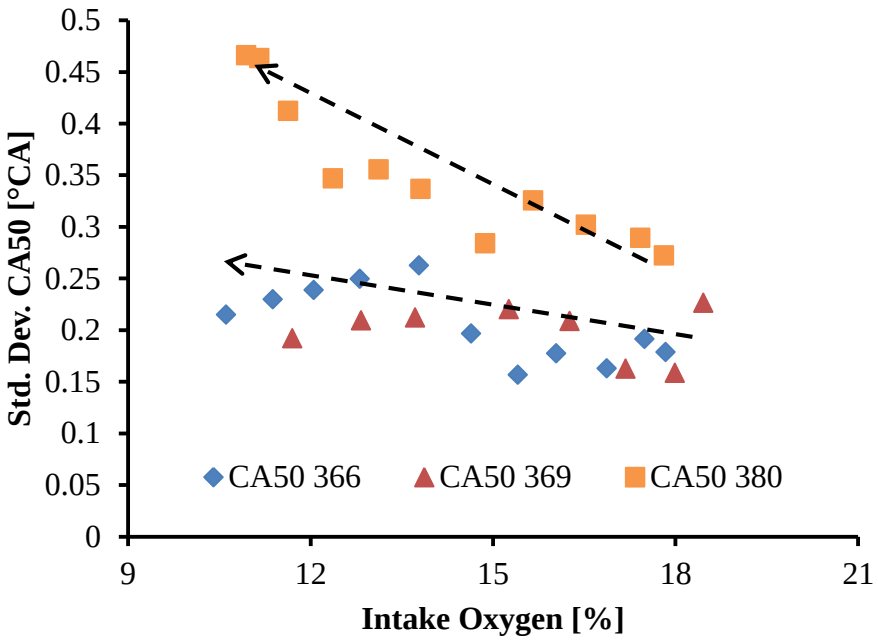

Figure 3-16 Influence of Intake Oxygen on Std. Dev. of CA50 at Medium Load

Shown in Figure 3-17 to Figure 3-20 are the 200 cycle pressure and heat release traces for the earliest combustion phasing case, CA50 366, and the latest combustion phasing, CA50 380, at their lowest and highest EGR ratios.

Illustrated in Figure 3-17 are the 200 consecutive cycles of pressure and HRR for the CA50 366 °CA case at an intake oxygen concentration of 17.8%, the mean, minimum, maximum, and variation of the combustion parameters are shown in Table 3-5. The HRR trace showed a two peak shape which meant there were two combustion modes occurring. The first peak was caused by premixed combustion or the auto-ignition of approximately stoichiometric local mixtures, the second was caused by diffusion combustion.

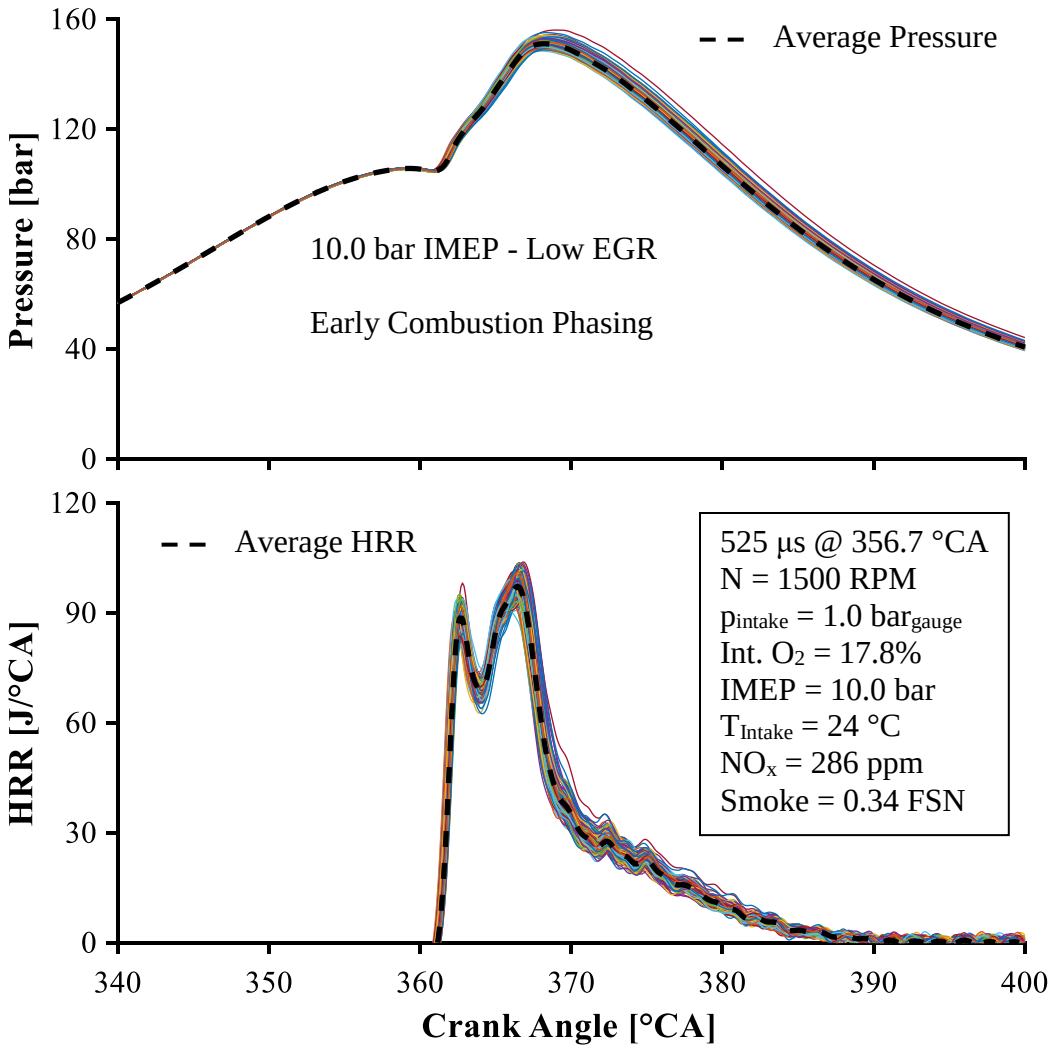

Figure 3-17 200 Cycle Pressure and HRR Trace of Low EGR Traditional Phasing

Table 3-5 Combustion Parameters of CA50 366 17.8% Intake Oxygen 200 Cycle Data

Parameter	Mean	Minimum	Maximum	Variation
p_{max}	151.0 bar	148.3 bar	156.0 bar	0.8%
IMEP	10.0 bar	9.3 bar	11.8 bar	3.7%
CA50	366.9 °CA	366.4 °CA	367.4 °CA	0.18 °CA

Depicted in Figure 3-18 are the 200 cycle traces of pressure and HRR for the minimum intake oxygen condition of the CA50 366 °CA test, which resulted in the production of 16 ppm NO_x and 5.0 FSN smoke. The mean, minimum, maximum, and variation of the combustion parameters are shown in

Table 3-6. With the application of EGR there was a merging of the premixed and diffusion combustion modes resulting in a single peak of heat release. This was caused by the increased mixing from the increased ignition delay. This resulted in a lower p_{max} and IMEP due to the suppression of peak temperature and incomplete combustion. However under reduced intake oxygen concentrations this test resulted in a reduction in variation of the p_{max} and IMEP which was contrary to literature findings [14, 17, and 18]. However, this could be related to larger periodic variations similar to those reported by Sen et al. [18], therefore the tests should be repeated, or a larger quantity of consecutive cycles should be recorded to investigate this.

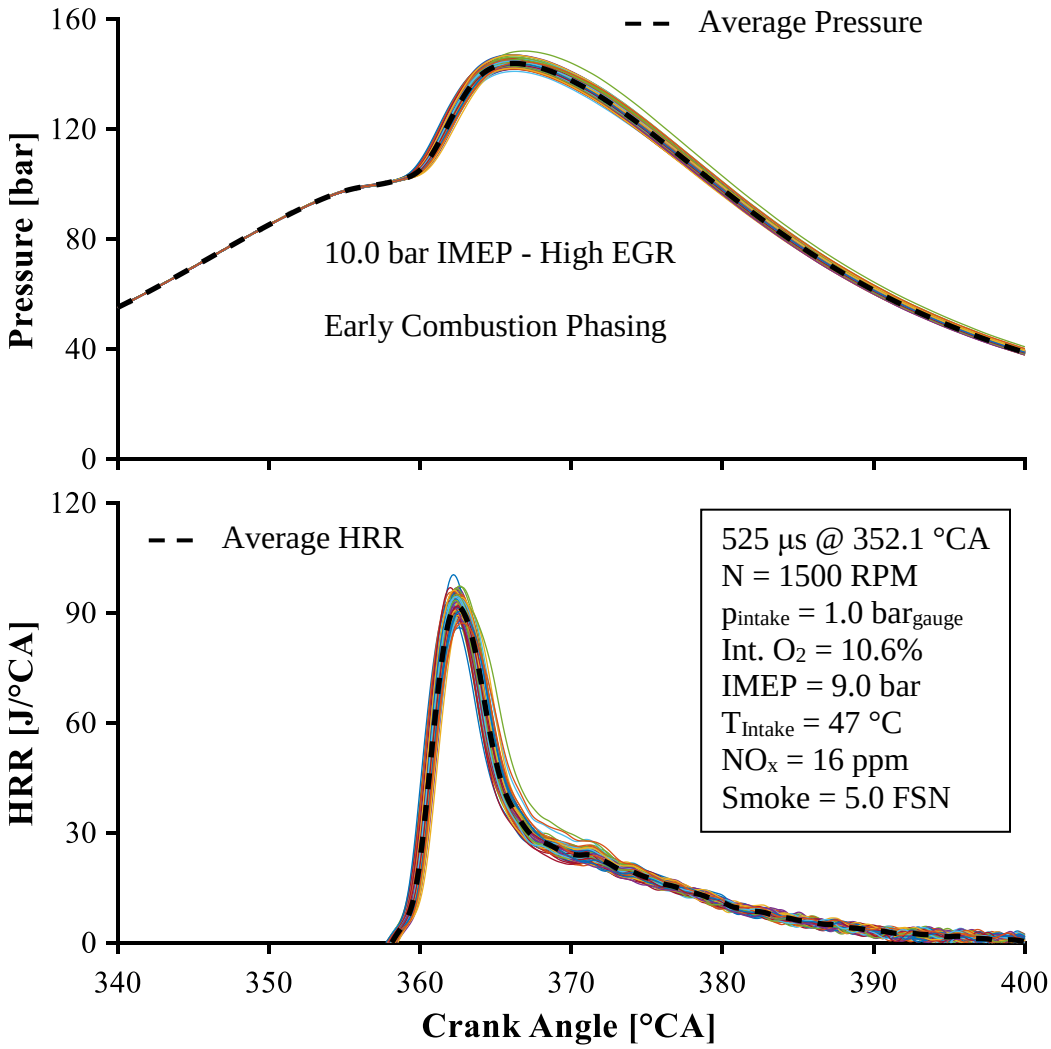

Figure 3-18 200 Cycle Pressure and HRR Trace High EGR Traditional Phasing

Table 3-6 Combustion Parameters of CA50 366 10.6% Intake Oxygen 200 Cycle Data

Parameter	Mean	Minimum	Maximum	Variation
p_{max}	143.8 bar	141.0 bar	148.3 bar	0.7%
IMEP	9.0 bar	8.5 bar	10.2 bar	2.8%
CA50	365.6 °CA	365.0 °CA	366.3 °CA	0.22 °CA

Illustrated in Figure 3-19 are the pressure and HRR traces of the CA50 380 °CA combustion phasing with an intake oxygen of 17.8%. The mean, minimum, maximum, and variation of the combustion parameters are shown in Table 3-7. Even at the highest intake oxygen concentration the HRR trace had a single peak because of the long ignition delay caused by the late combustion phasing, resulting in a large portion of the combustion being of the premixed type. Additionally, the very late combustion phasing resulted in the p_{max} due to combustion being lower than the maximum motoring pressure. The COV_{IMEP} is lower for this test condition than the highest and lowest intake oxygen for test with a CA50 of 366 °CA. This could be because of the relatively much lower peak in-cylinder temperature resulting in consistently supressed combustion represented by the large quantities of incomplete combustion products, or it could be related to periodic variation throughout engine operation similar to those reported in literature [18].

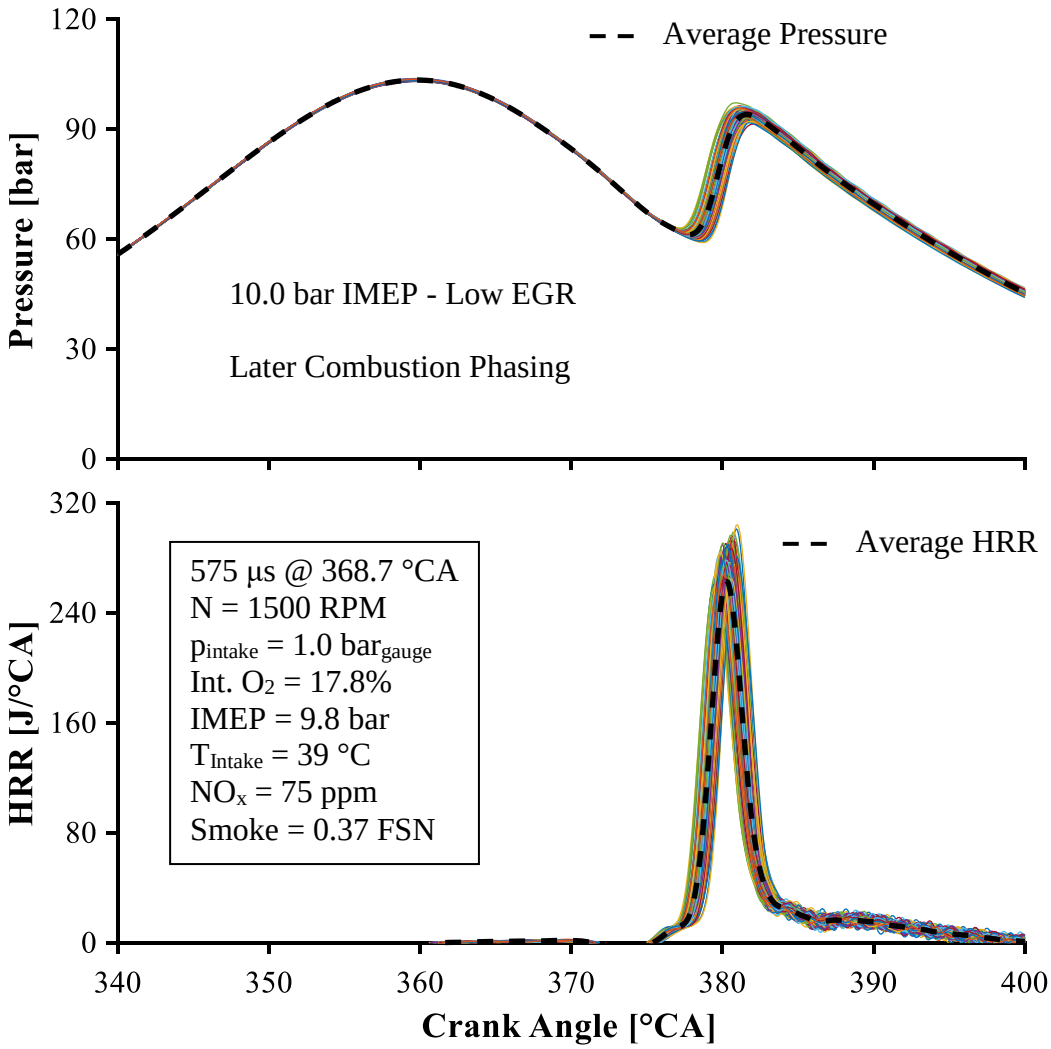

Figure 3-19 200 Cycle Pressure and HRR Trace Low EGR Late Phasing

Table 3-7 Combustion Parameters of CA50 380 17.8% Intake Oxygen 200 Cycle Data

Parameter	Mean	Minimum	Maximum	Variation
p_{max}	93.9 bar	91.3 bar	97.1 bar	1.0%
IMEP	9.8 bar	9.3 bar	10.2 bar	2.1%
CA50	380.7 °CA	380.0 °CA	381.3 °CA	0.28 °CA

Shown in Figure 3-20 are 200 consecutive cycles of pressure and HRR for the lowest intake oxygen condition for the CA50 380 °CA test. The mean, minimum, maximum, and variation of the combustion parameters are shown in Table 3-8. Both the pressure and HRR traces show considerably more variation than the 17.8% intake oxygen test, this was represented most obviously by the significant increase in COV_{pmax} but only marginally reflected with the slight increase in COV_{IMEP}.

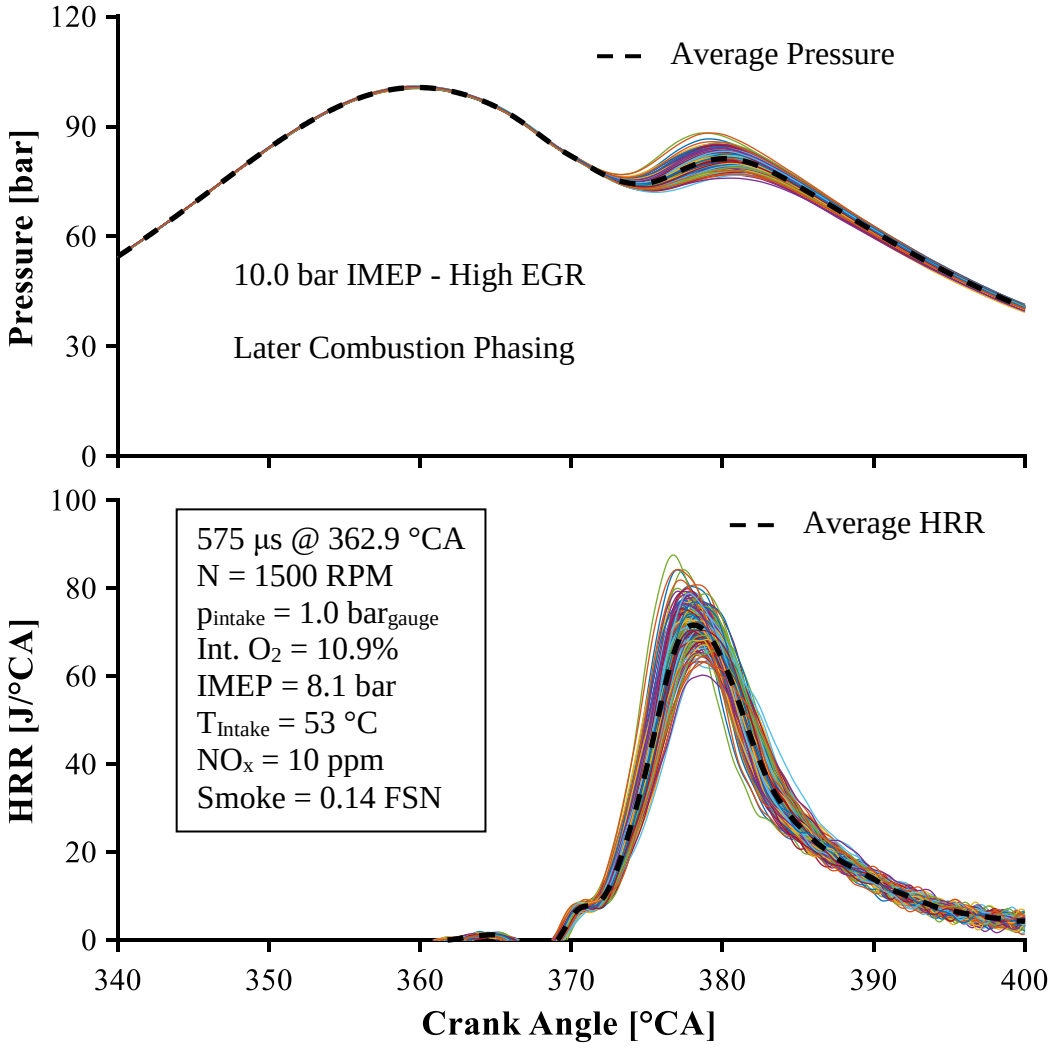

Figure 3-20 200 Cycle Pressure and HRR Trace High EGR Late Phasing

Table 3-8 Combustion Parameters of CA50 380 10.9% Intake Oxygen 200 Cycle Data

Parameter	Mean	Minimum	Maximum	Variation
p_{max}	81.3 bar	75.9 bar	88.2 bar	2.6%
IMEP	8.1 bar	7.5 bar	8.6 bar	2.3%
CA50	380.1 °CA	378.6 °CA	381.3 °CA	0.26 °CA

With the reduction of intake oxygen from approximately 18% to 11% there was a significant reduction in the p_{max} and IMEP for both test cases shown above. When the CA50 was shifted from 366 to 380 °CA, the heat release shape changed from a double to a single peak, this effect was also obtained by reducing the intake oxygen concentration. The transition to a single peak of HRR represented an increase in the quantity of premixed combustion and a merging of the premixed and diffusion combustion modes. When a combination of EGR and late combustion phasing was applied there was a significant increase in the combustion duration.

3.3 Chapter Summary

The effect of EGR and combustion phasing on diesel combustion was reported in this chapter.

At all engine loads and combustion phasing EGR was effective at reducing NO_x emissions, this came at the expense of an increase in smoke emissions. However for the 3.5 bar IMEP test and the 10 bar IMEP test with a CA50 of 380 °CA once intake oxygen was reduced to below 13% there was a reduction in soot emissions. Both of these tests resulted in a

simultaneous reduction of smoke and NO_x emissions, although only the 380 CA50 accomplished LTC, identified by the ultra-low NO_x and soot emissions.

By retarding combustion phasing it was possible to reduce peak NO_x production as well as peak smoke along with obtaining LTC.

Kyrtatos et al. [14 & 17] and Koizumi et al. [16] reported that with the application of EGR or an increase in the premixed portion of combustion there was an increase in the COV_{IMEP}, however only the 3.5 bar IMEP followed this trend, but only occurred at intake oxygen levels less than 13%. All other tests investigated had no clear trend between the COV_{IMEP} and the intake oxygen concentration. The tests should be repeated to confirm that this is not an anomaly, if it does not appear to be an anomaly then the contrary results may be due to the different test setups.

With the retarding of combustion phasing there was a decrease in the COV_{IMEP} for the 10 bar IMEP cases investigated. The reduction in the COV_{IMEP} could be because at early combustion phasing timings the diffusion combustion mode was strongly affected by changes in the background in-cylinder conditions. Whereas the late combustion phasing was primarily premixed type combustion which was more repeatable as a result of the longer mixing time.

The standard deviation of CA50 had a similar trend for all tests – an increase with decreasing intake oxygen concentration. The most significant increase occurred for the 10 bar IMEP test with a CA50 of 380 °CA.

CHAPTER 4: DIESEL DI ETHANOL PFI COMBUSTION

Demonstrated in this chapter will be the dual fuel combustion using port injected ethanol and direct injected diesel tests. Ethanol was port injected as it has high resistance to auto-ignition, octane number 110 – 115, low boiling temperature, 78°C, and high latent heat of evaporation, 728.2 kJ/kg, as shown in Table 2-3. Reported in the first section of this chapter are the results from the EGR sweep tests on different diesel – ethanol ratios. Shown in the following section is a comparison of the lowest NO_x emission from the previous chapter and select diesel – ethanol ratios, finally the effect of injection timing on micro-injection diesel and ethanol combustion are presented.

4.1 Influence of EGR on Different Diesel – Ethanol Ratios

The test conditions shown in Table 4-1 are for EGR sweeps of five different diesel – ethanol fuel ratios and a diesel only test. The diesel direct injection timing was adjusted to maintain a constant CA50 at approximately 368 °CA for all test conditions. The intake pressure, engine speed, direct injection pressure, port injection pressure, and port injection timing were kept constant for all cases. The cases were defined based on the quantity of load produced by each fuel. For instance the D60:E40 case had 6 bar IMEP contributed from diesel fuel and 4 bar produced from ethanol fuel for a total of 10 bar IMEP.

Table 4-1 Diesel Direct Injection Ethanol Port Injection Combustion Test Matrix

	D100:E0	D80:E20	D60:E40	D40:E60	D20:E80	D5:E95
DI Inj. Timing [°CA]	358.2 – 354.5	358.0 – 354.6	368.0 – 353.8	358.0 – 352.0	358.0 – 350.0	355.0 – 344.0
DI Inj. Duration [μs]	610	520	450	380	330	270
DI Inj. Pressure [bar]	1200	1200	1200	1200	1200	900
PFI Inj. Timing [°CA]	10	10	10	10	10	10
PFI Inj. Duration [μs]	0	2100	2600	3400	4200	5650
PFI Inj. Pressure [bar]	8	8	8	8	8	8
T_{Intake} [°C]	30 – 36	33 - 37	30 – 40	30 – 42	33 – 42	26 – 49
p_{Intake} [bar]	1.0	1.0	1.0	1.0	1.0	1.0
Engine Speed [rpm]	1500	1500	1500	1500	1500	1500
Intake Oxygen [%]	19.8 – 13.2	19.0 – 13.1	19.3 – 12.5	19.6 – 11.6	19.8 – 12.3	20.7 – 13.7
IMEP [bar]	10.3 – 9.6	10.3 – 9.9	10.0 – 9.7	10.3 – 9.4	10.8 – 9.8	10.5 – 7.2
CA50	367.1 – 368.9	367.6 – 368.6	367.4 – 368.7	367.9 – 369.2	367.8 – 369.3	373.4 – 368.0

Shown in Figure 4-1 is the effect of intake oxygen concentration on NO_x emissions for different diesel – ethanol ratios. At the highest intake oxygen concentration there was an immediate reduction of NO_x emissions with the addition of ethanol. The NO_x emissions reduced from over 900 ppm to less than 450 ppm for all cases when some ethanol fuel was injected. In all cases there was a reduction in NO_x emissions with the application of EGR. Once the intake oxygen concentration was reduced to 15%, the NO_x emissions were less than 100 ppm for all cases, this might be caused by the suppression of the auto-ignition of the diesel fuel allowing more time for mixing.

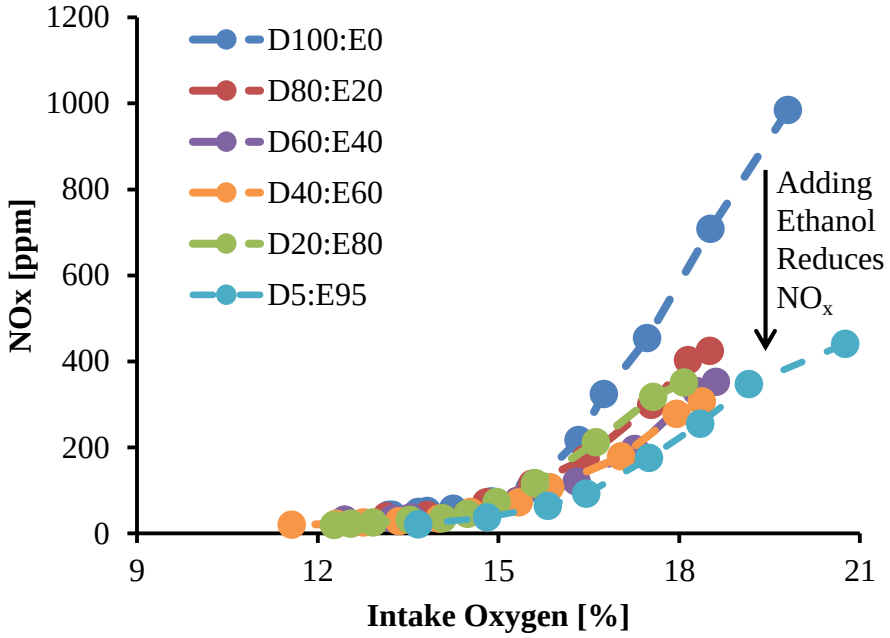

Figure 4-1 Effect of Intake Oxygen on NO_x Emissions for Medium Load Dual Fuel

The effect of EGR on smoke emissions is shown in Figure 4-2. A similar trend is seen to the diesel single shot cases shown in the previous chapter Figure 3-2 and Figure 3-11, an increase in smoke emissions with the dilution of some of the fresh air with exhaust products. Two out of the six cases did not have an increase in smoke emissions with reduced intake oxygen, the exceptions being D20:E80 and D5:E95. For the D20:E80 and D5:E95 cases the majority of the energy was supplied by port injection therefore a homogeneous mixture was formed in the cylinder which was then ignited by a small quantity of diesel. The combustion of this homogenous mixture resulted in low smoke emissions for all intake oxygen concentrations.

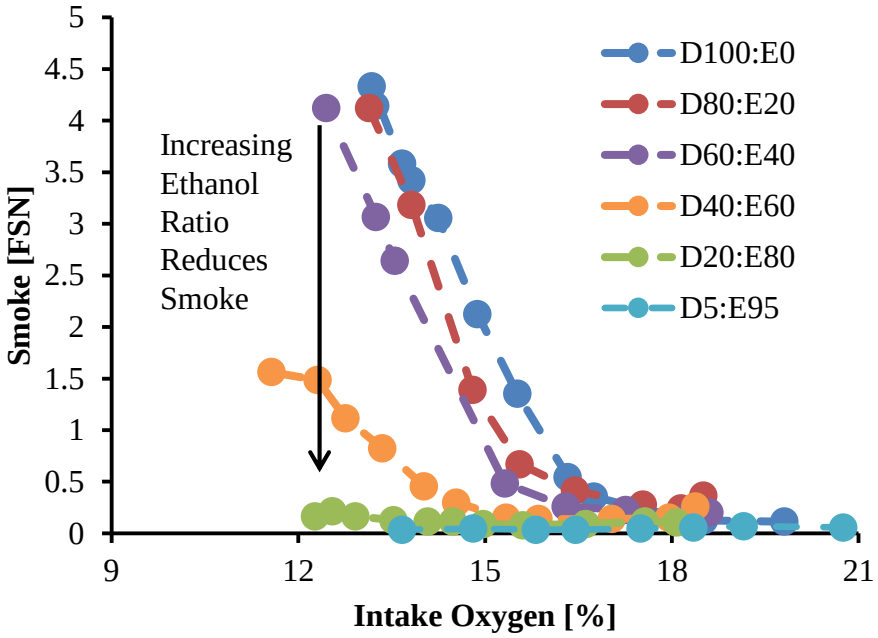

Figure 4-2 Effect of Intake Oxygen on PM Emissions for Medium Load Dual Fuel

The negligible effect of EGR on particulate matter emissions in the D20:E80 and D5:E95 cases means that the traditional NO_x – Soot trade-off was not a concern for this dual fuel RCCI strategy. A possible reason for this was the fact that a sufficient portion of the combustion occured in the premixed combustion regime.

The influence of intake oxygen on the IMEP is shown in Figure 4-3. The overall effect of intake oxygen on IMEP was similar to the diesel single shot case shown in Figure 3-12, a reduction in IMEP as intake oxygen reduces, however the reduction was much less significant for the dual fuel tests. The exception to this is the D5:E95 case, where the reduction of intake oxygen from 14.8% to 13.7% resulted in a reduction in IMEP from 10.0 to 7.3 bar.

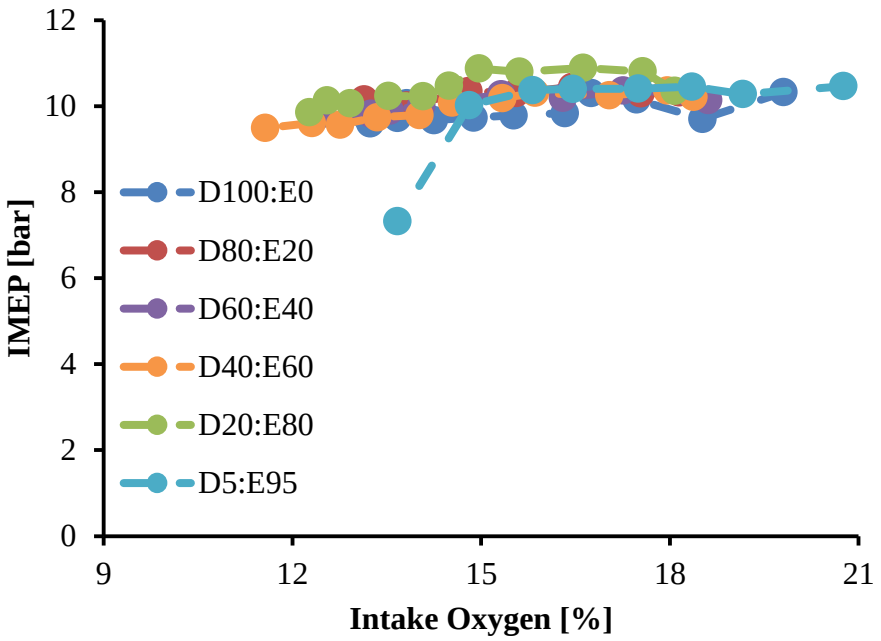

Figure 4-3 Effect of Intake Oxygen on IMEP for Medium Load Dual Fuel

Presented in Figure 4-4 is the effect of EGR on the COV_{IMEP}. The COV_{IMEP} was largely independent of intake oxygen concentration for diesel – ethanol ratios of D100:E0, D80:E20, D60:E40, and D40:E60. For most intake oxygen concentrations the COV_{IEP} was highest for the D5:E95 however it was below 2.5% for all but the lowest intake oxygen concentration, 13.7%. For the D5:E95 test when the intake oxygen was reduced from 14.8% to 13.7% intake oxygen there was a dramatic increase in the COV_{IMEP} to 16%. A possible reason for this is the suppression of the ignition of the diesel injection which was used as the ignition source, and caused unreliable ignition timing resulting in high fluctuation of IMEP and CA50. There could also be variation in the combustion of the ethanol – air mixture after the diesel direct injection caused by the variation in the background conditions in the cylinder.

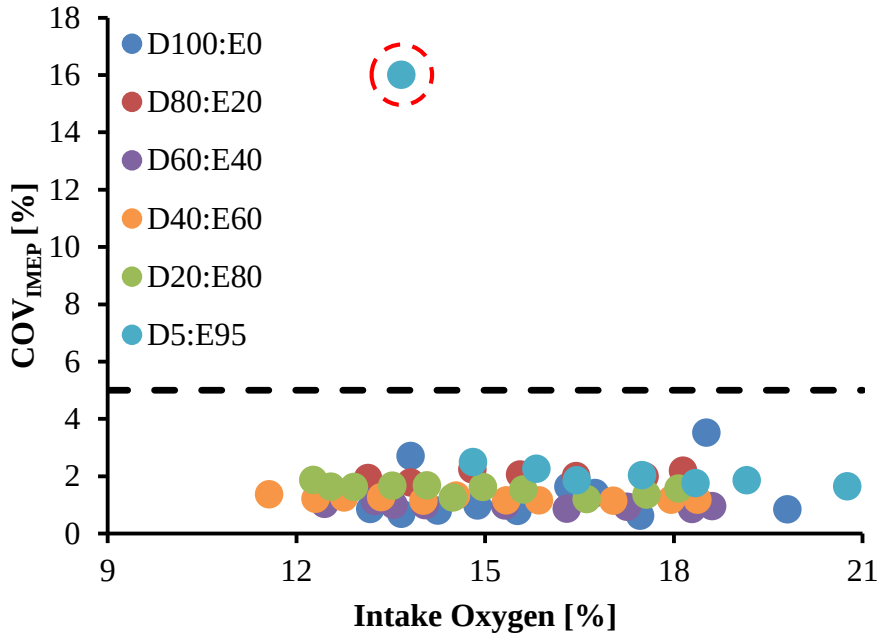

Figure 4-4 Effect of Intake Oxygen on COV_{IMEP} for Medium Load Dual Fuel

The effect of reducing intake oxygen concentration on the standard deviation of CA50 for the different diesel – ethanol ratios is shown in Figure 4-5. With increasing ethanol fraction there was a greater variation in CA50 for all intake oxygen concentrations. All tests resulted in an increase in the standard deviation of CA50 with decreasing intake oxygen. Intake oxygen concentration had minimal effect on the standard deviation of CA50 of the D100:E0 case. The standard deviation of CA50 increased linearly with decreasing intake oxygen for the D80:E20, D60:E40, and D40:E60 tests. The D20:E80 case had a linear increase from 18 to 15% intake oxygen, and then an exponential increase from 15 to 12% intake oxygen. The standard deviation of CA50 was highest for the D5:E95 test for all intake oxygen concentrations. Similar to the D20:E80 test the D5:E95 had a linear increase in the standard deviation of CA50 when the intake oxygen was reduced from 21% to 14.8%, however when the intake oxygen concentration was further reduced to 13.7% the standard deviation of CA50 increased from 0.5 to 1.1 °CA.

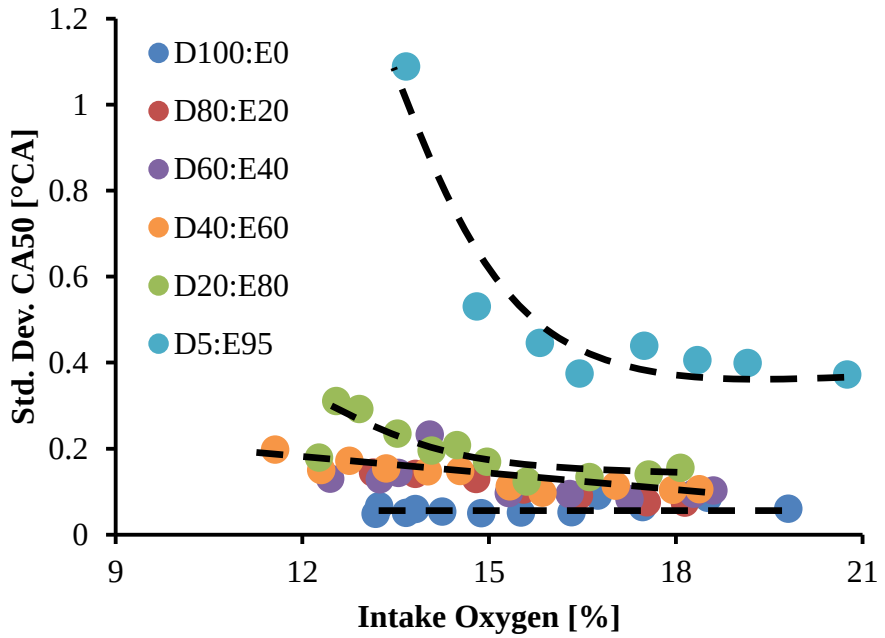

Figure 4-5 Effect of Intake Oxygen on Std. Dev. of CA50 for Medium Load Dual Fuel

Illustrated in the following figures, Figure 4-6 to Figure 4-11, are the 200 consecutive cycle pressure and heat release traces for D100:E0, D20:E80, and D5E:95 at their highest and lowest intake oxygen concentrations respectively. Only the D20:E80 and D5:E95 diesel – ethanol ratios are shown as only these two tests were able to achieve simultaneously low NO_x and PM emissions.

First the diesel only case at 19.8% intake oxygen is presented in Figure 4-6. No significant deviation from the average value was observed. The mean, minimum, maximum, and variation of the combustion parameters are shown in Table 4-2. As seen in the previous chapter there was a two peak heat release shape, which represents a premixed and a diffusion combustion mode. The diffusion zone was considerably larger than the premixed zone, which resulted in higher combustion temperatures and therefore more NO_x emissions.

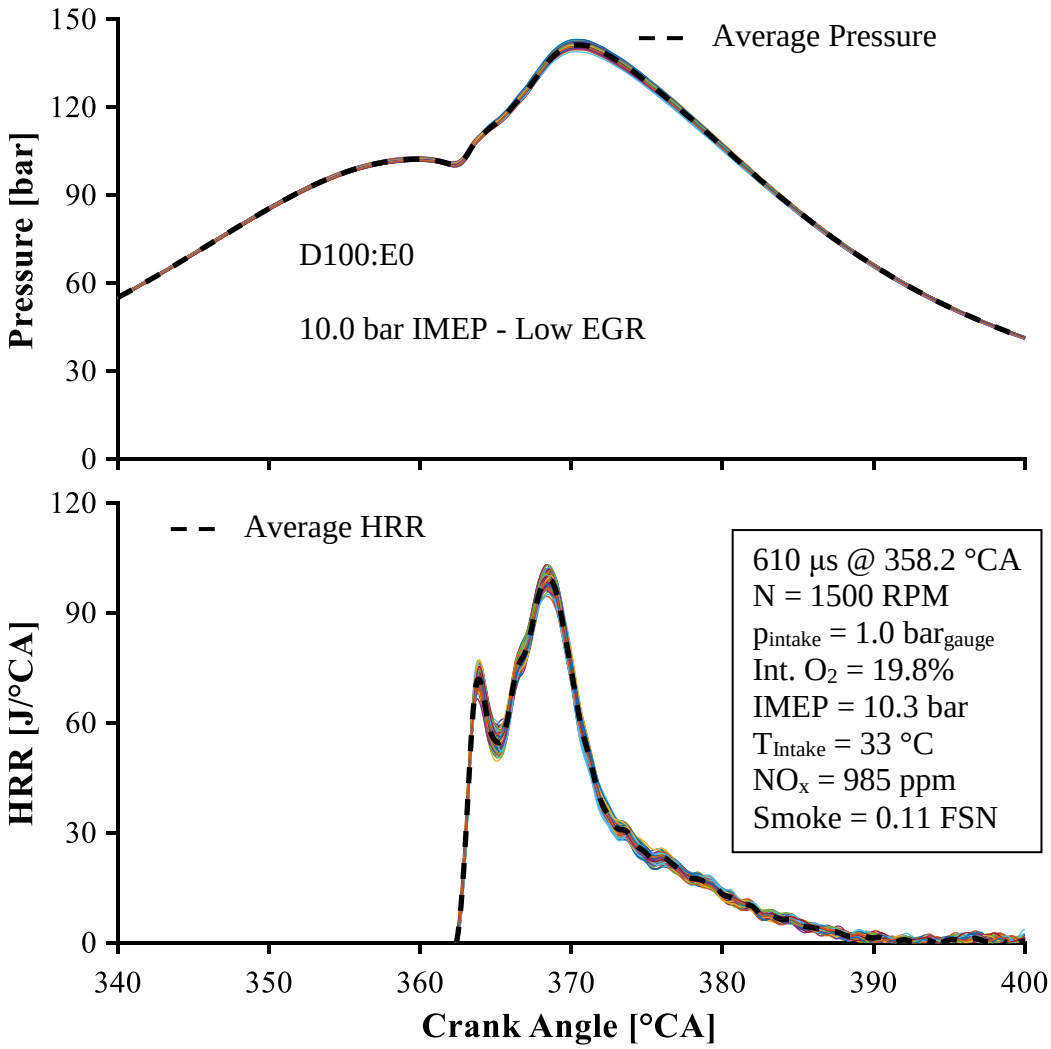

Figure 4-6 200 Cycle Pressure and HRR Trace for 19.8% Intake Oxygen D100:E0

Table 4-2 Combustion Parameters of D100:E0 19.8% Intake Oxygen 200 Cycle Data

Parameter	Mean	Minimum	Maximum	Variation
p_{max}	141.1 bar	138.8 bar	143.0 bar	0.4%
IMEP	10.3 bar	10.1 bar	10.5 bar	0.8%
CA50	369.0 °CA	368.8 °CA	369.1 °CA	0.06 °CA

Shown in Figure 4-7 are the 200 consecutive cycle pressure and HRR traces for the D100:E0 case at 13.2% intake oxygen. The pressure and HRR traces show more deviation from the mean than Figure 4-6, the 19.8% intake oxygen case. The mean, minimum, maximum, and variation of the combustion parameters are shown in Table 4-3. With the reduction of intake oxygen, it was observed that the two combustion zones merged closer together and that a greater portion of the combustion was of the premixed type. An increase in the premixed combustion mode resulted in a lower peak temperature, and therefore lower NO_x production. However, as there is less oxygen available after combustion less oxidation of particulates occurred, which resulted in high smoke emissions.

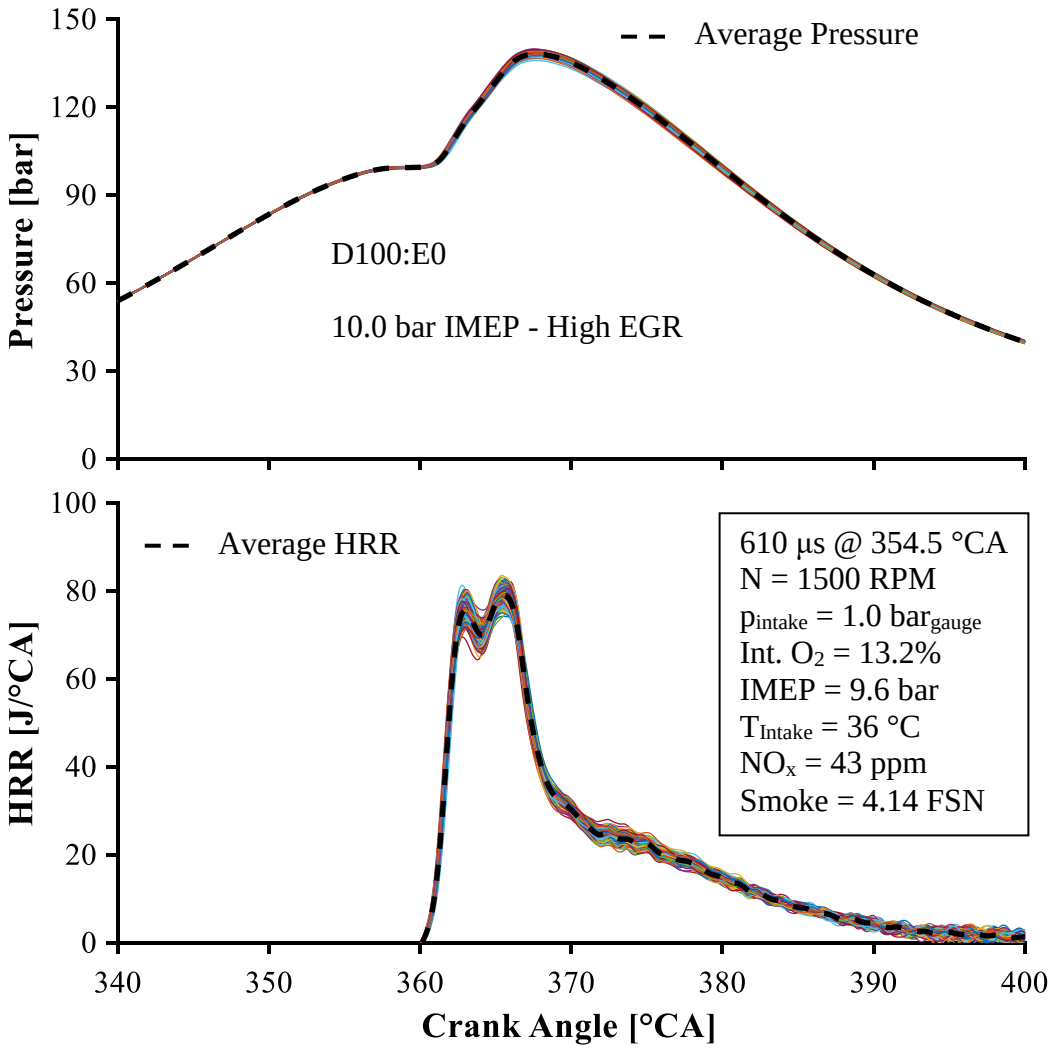

Figure 4-7 200 Cycle Pressure and HRR Trace for 13.2% Intake Oxygen D100:E0

Table 4-3 Combustion Parameters of D100:E0 13.2% Intake Oxygen 200 Cycle Data

Parameter	Mean	Minimum	Maximum	Variation
p_{max}	138.1 bar	135.9 bar	139.8 bar	0.5%
IMEP	9.6 bar	9.3 bar	9.9 bar	1.1%
CA50	367.4 °CA	367.1 °CA	367.8 °CA	0.07 °CA

Illustrated in Figure 4-8 are the 200 cycle pressure and HRR traces for the D20:E80 test with an intake oxygen concentration of 18.1%. Considerably more variation can be seen in the curves compared to the D100:E0 case at either of the two intake oxygen concentrations shown previously in Figure 4-6 and Figure 4-7. The mean, minimum, maximum, and variation of the combustion parameters are shown in Table 4-4. As the majority of the supplied fuel energy is from the ethanol port injected fuel, the heat release shape of the premixed portion of combustion had a larger magnitude than the diffusion part. This resulted in a lower peak temperature and therefore less NO_x emissions compared to the D100:E0 test at 19.8% intake oxygen concentration.

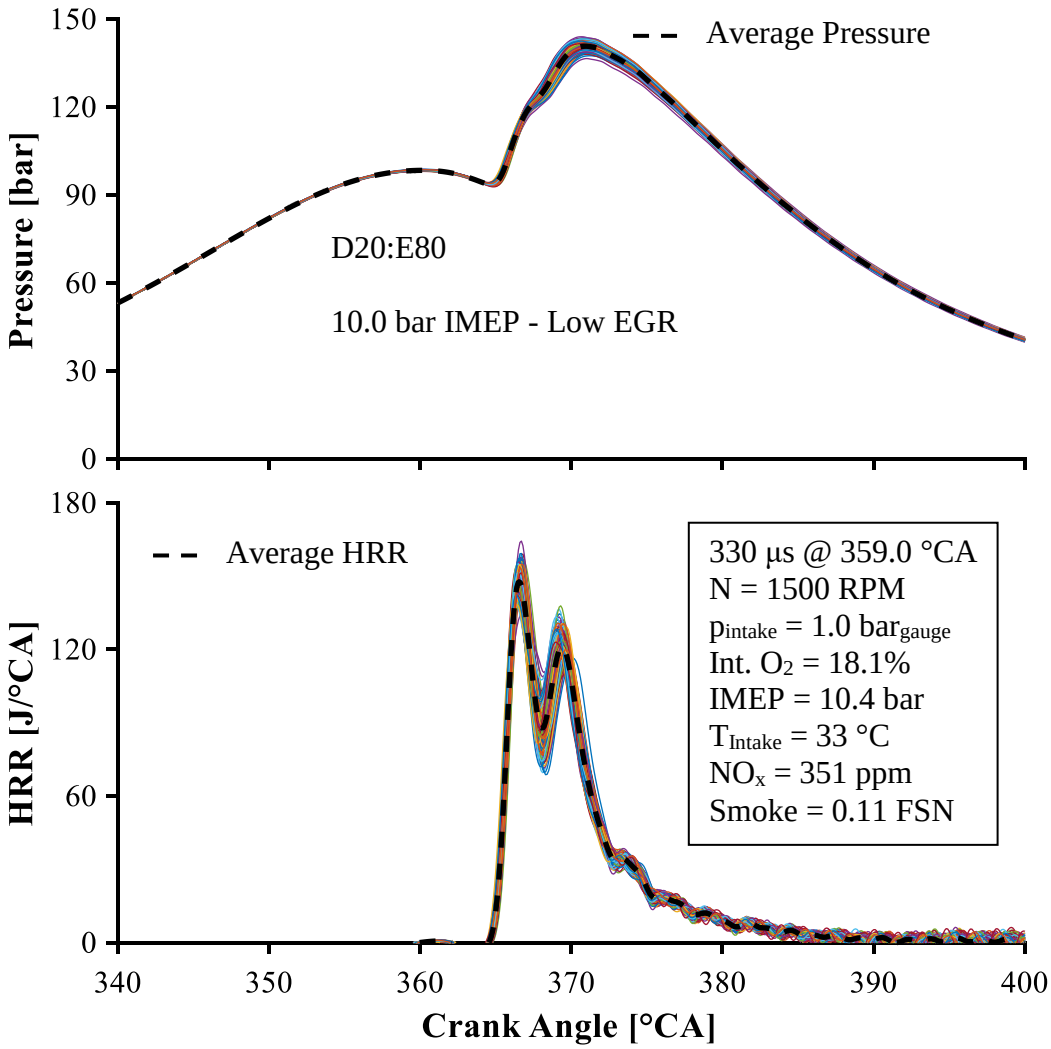

Figure 4-8 200 Cycle Pressure and HRR Trace for 18.1% Intake Oxygen D20:E80

Table 4-4 Combustion Parameters of D20:E80 18.1% Intake Oxygen 200 Cycle Data

Parameter	Mean	Minimum	Maximum	Variation
p_{max}	140.8 bar	136.5 bar	144.0 bar	0.4%
IMEP	10.4 bar	9.9 bar	10.9 bar	1.1%
CA50	369.3 °CA	368.9 °CA	369.8 °CA	0.16 °CA

Shown in Figure 4-9 are the 200 cycle pressure and HRR traces respectively for the D20:E80 with an intake oxygen of 12.3%. More variation in the pressure and HRR traces can be seen at these conditions, especially close to the peak of HRR. The mean, minimum, maximum, and variation of the combustion parameters are shown in Table 4-5. At these conditions it is not possible to distinguish the premixed and diffusion combustion zones, but it is assumed that the majority of the combustion was of the premixed type, because it has been reported in literature that with the application of EGR there was an increase in mixing time [25].

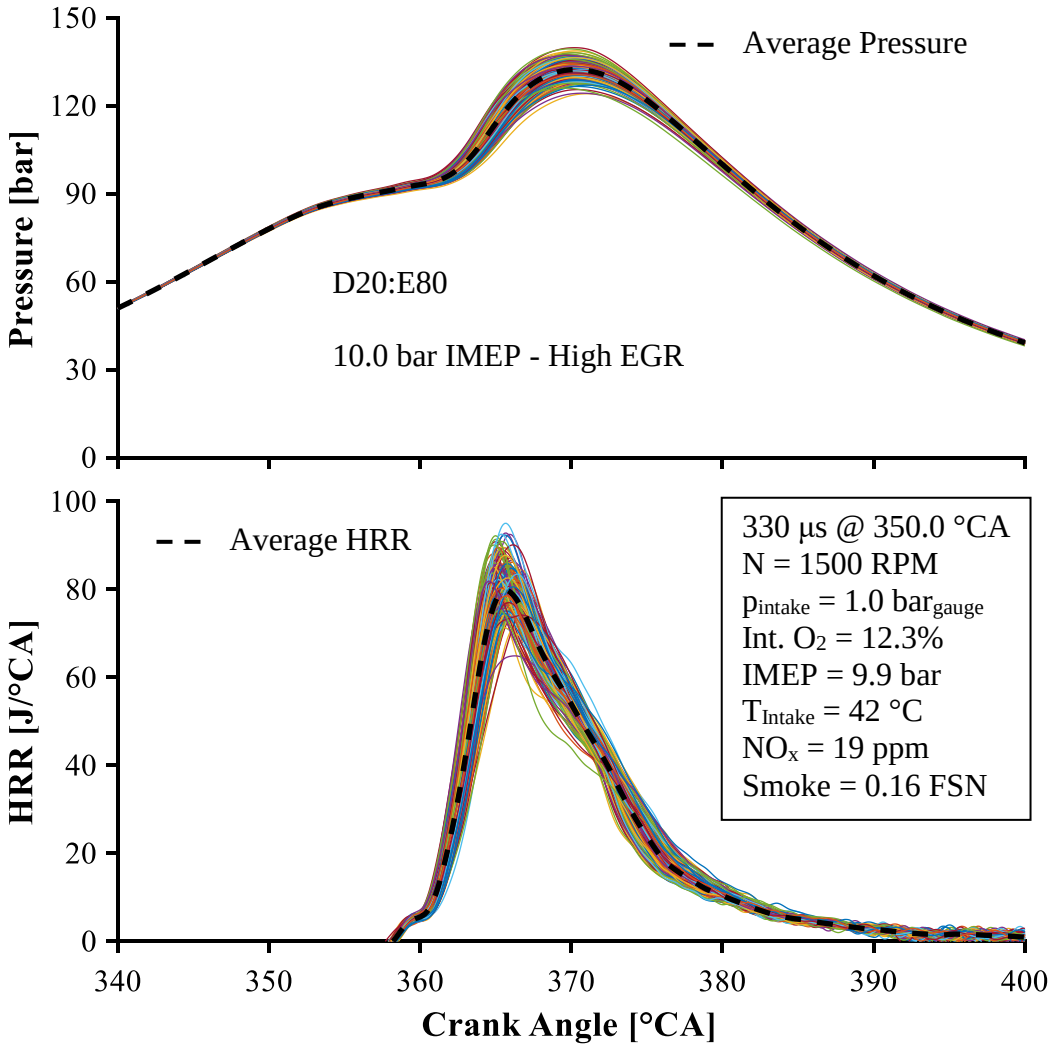

Figure 4-9 200 Cycle Pressure and HRR Trace for 12.3% Intake Oxygen D20:E80

Table 4-5 Combustion Parameters of D20:E80 12.3% Intake Oxygen 200 Cycle Data

Parameter	Mean	Minimum	Maximum	Variation
p_{max}	132.3 bar	124.1 bar	139.8 bar	1.0%
IMEP	9.9 bar	9.2 bar	10.4 bar	1.6%
CA50	366.9 °CA	366.4 °CA	367.4 °CA	0.18 °CA

Shown in Figure 4-10 are the 200 cycle pressure and HRR traces respectively for the D5:E95 with an intake oxygen concentration of 20.7%. The mean, minimum, maximum, and variation of the combustion parameters are shown in Table 4-6. Larger variation in both the pressure and HRR traces can be seen in Figure 4-10 compared to Figure 4-6 to Figure 4-9. At these conditions the two hump HRR shape was reflected in the pressure trace. The HRR trace appears to be diffusion dominated because the second peak is larger than the first, and the second zone is usually considered to be diffusion combustion [25]. Thisis unexpected as 95% of the fuel energy is homogenously mixed with air. Therefore, it might not be appropriate to consider the first and second peaks as premixed and diffusion combustion zones for this diesel – ethanol ratio.

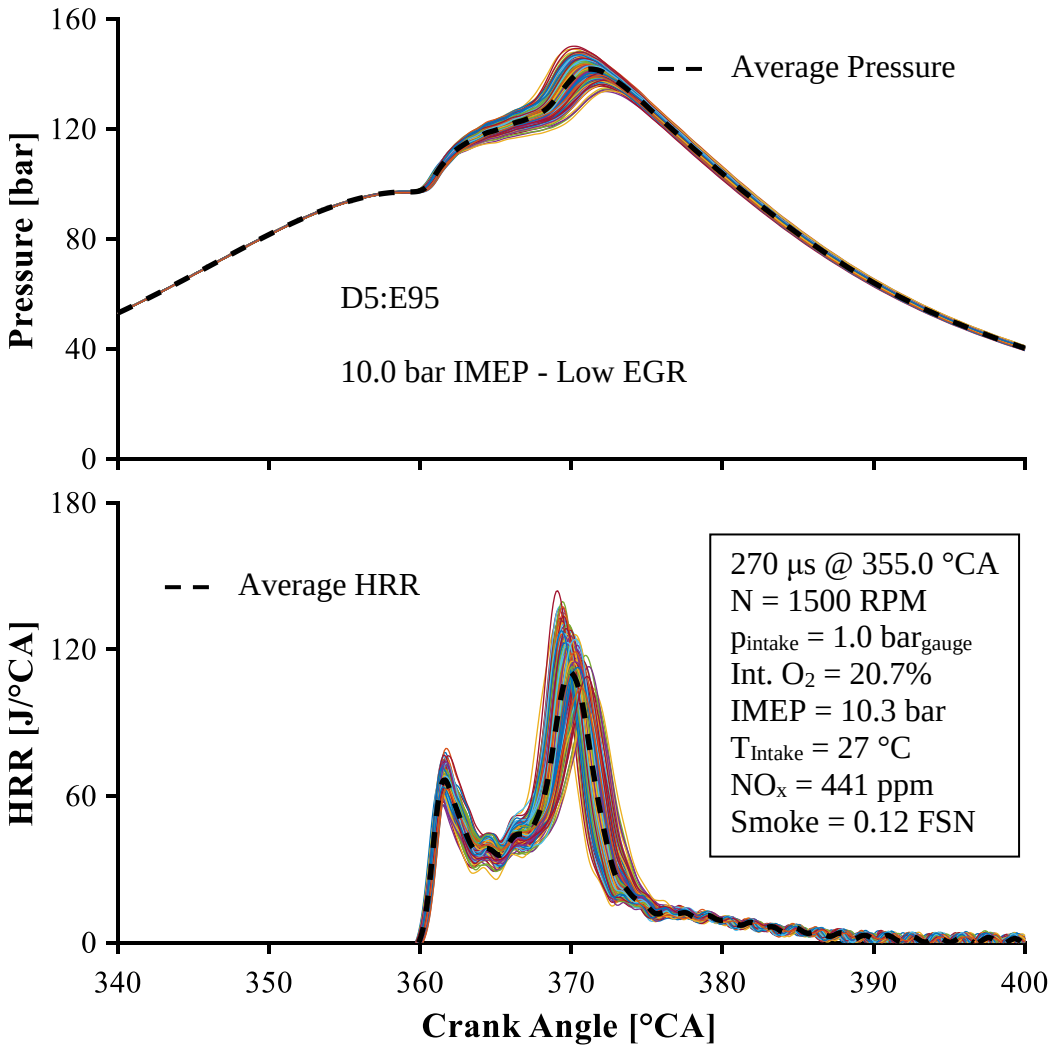

Figure 4-10 200 Cycle Pressure and HRR Trace for 20.7% Intake Oxygen D5:E95

Table 4-6 Combustion Parameters of D5:E95 20.7% Intake Oxygen 200 Cycle Data

Parameter	Mean	Minimum	Maximum	Variation
p_{max}	142.3 bar	133.6 bar	150.1 bar	1.9%
IMEP	10.3 bar	9.7 bar	10.8 bar	1.6%
CA50	369.3 °CA	368.3 °CA	370.5 °CA	0.37 °CA

Shown in Figure 4-11 are the 200 cycle pressure and HRR traces for the D5:E95 test with an intake oxygen of 13.7%. The mean, minimum, maximum, and variation of the combustion parameters are shown in Table 4-7. The variation in the pressure and HRR traces was the greatest of these tests, Figure 4-6 to Figure 4-11, as would be expected from the high COV_{IMEP} and standard deviation of CA50. Similar to the D20:E80 test at low oxygen conditions, the diffusion and premixed zones have merged together. The ignition delay of the diesel injection increased from 7.4 to 18.5 °CA when the intake oxygen concentration was reduced from 20.7% to 13.7%, this resulted in improved mixing and in a lowered peak cylinder temperature, and therefore reduced NO_x emissions.

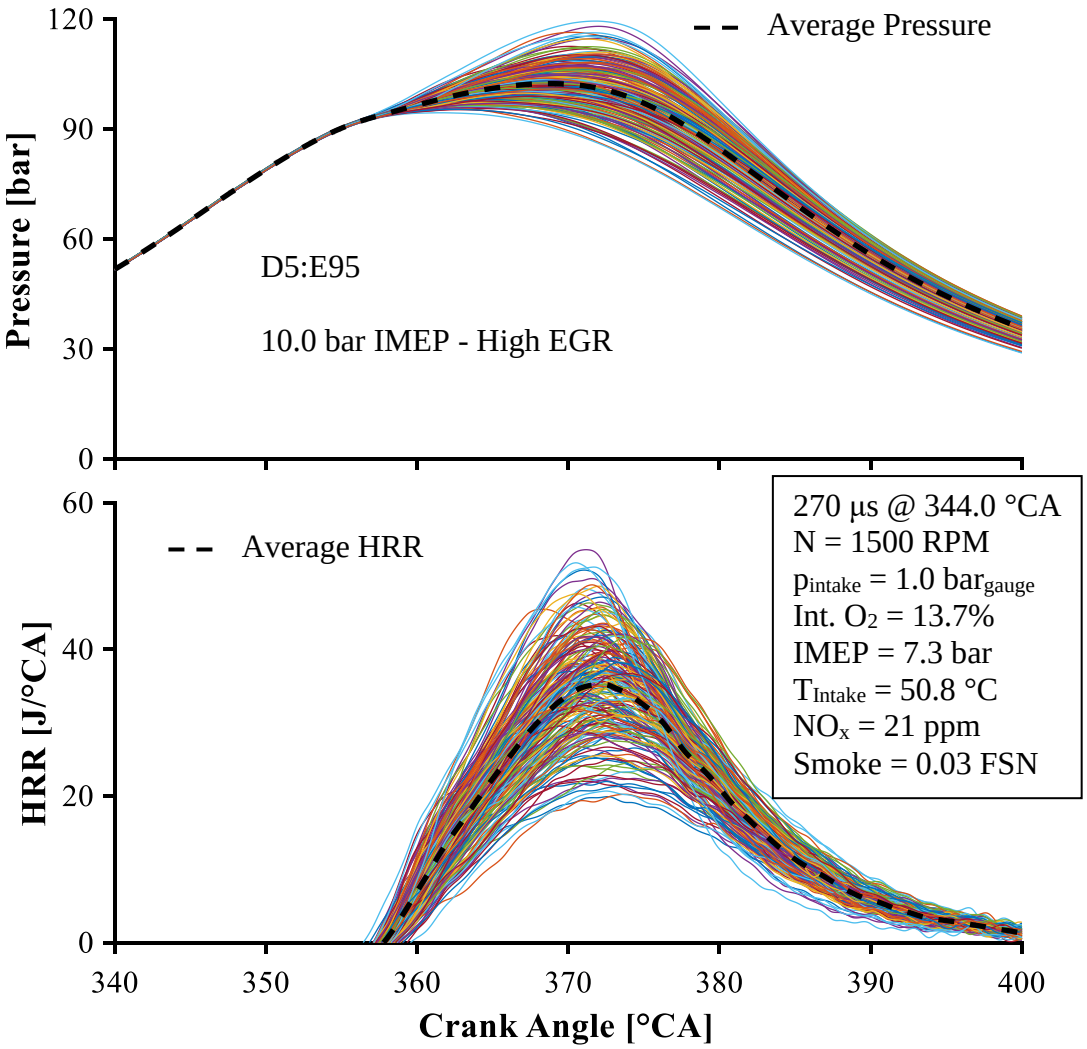

Figure 4-11 200 Cycle Pressure and HRR Trace for 13.7% Intake Oxygen D5:E95

Table 4-7 Combustion Parameters of D5:E95 13.7% Intake Oxygen 200 Cycle Data

Parameter	Mean	Minimum	Maximum	Variation
p_{max}	103.4 bar	94.4 bar	119.4 bar	4.8%
IMEP	7.3 bar	3.7 bar	9.2 bar	16.0%
CA50	369.3 °CA	367.8 °CA	370.7 °CA	1.1 °CA

4.2 Lowest NO_x Result Comparison

Shown in this section is the comparison of the lowest NO_x conditions for the diesel single shot CA50 380 °CA timing (shown in the previous chapter), D60:E40, D20:E80, and D5:E95 tests. The smoke, CO, and THC emissions, as well as the COV_{IMEP}, and the standard deviation of CA50 obtained for each test are presented. The intake oxygen concentrations and the NO_x emissions of each tests are shown in Table 4-8, also The NO_x emissions are written above the top left chart in Figure 4-12.

Table 4-8 Intake Oxygen Concentration to Reach Lowest NO_x Emission

Test	Diesel CA50 380	D60:E40	D20:E80	D5:E95
Intake Oxygen [%]	10.9	12.5	12.3	13.7
NO_x [ppm]	10	32	19	21

The smoke was highest for the D60:E40 condition as the majority of the energy is contributed by the diesel direct injection, and there is still considerable diffusion combustion resulting in high smoke emissions. The measured smoke emissions of the CA50 380 and the D20:E80 tests were both below 0.2 FSN. However, the D5:E95 test had the lowest smoke: less than 0.05 FSN.

The measurement of CO emissions for the CA50 380 and D60:E40 tests were over 5000 ppm which saturated the analyser. The next highest CO emission was observed from the D5:E95 test with approximately 4800 ppm. The D20:E80 test had the lowest measured CO emissions with 3105 ppm.

The measured THC emissions were highest for the D5:E95 test at 3005 ppm. The D20:E80 test had the second highest THC emissions with a measurement of 1866 ppm. The D60:E40 and the CA50 380 tests had similar THC emissions with values of 1164 and 1061 ppm respectively.

The variation of IMEP and CA50 was the greatest for the D5:E95 condition, where the COV_{IMEP} was 16%. This was 6 times greater than the next highest $COV_{IMEP.}$ The standard deviation of CA50 of the D5:E95 test was 1.1 °CA, approximately double the second highest deviation of CA50. The COV_{IMEP} for all other tests was less than 3%, with the lowest variation being for the D60:E40 test. The standard deviation of the D60:E40 and D20:E80 tests were less than 0.2 °CA. The standard deviation of CA50 for the CA50 380 test was 0.47 °CA.

The best compromise of the smoke, CO, and THC emissions, and the COV_{IMEP} and standard deviation of CA50 was obtained for the D20:E80 test.

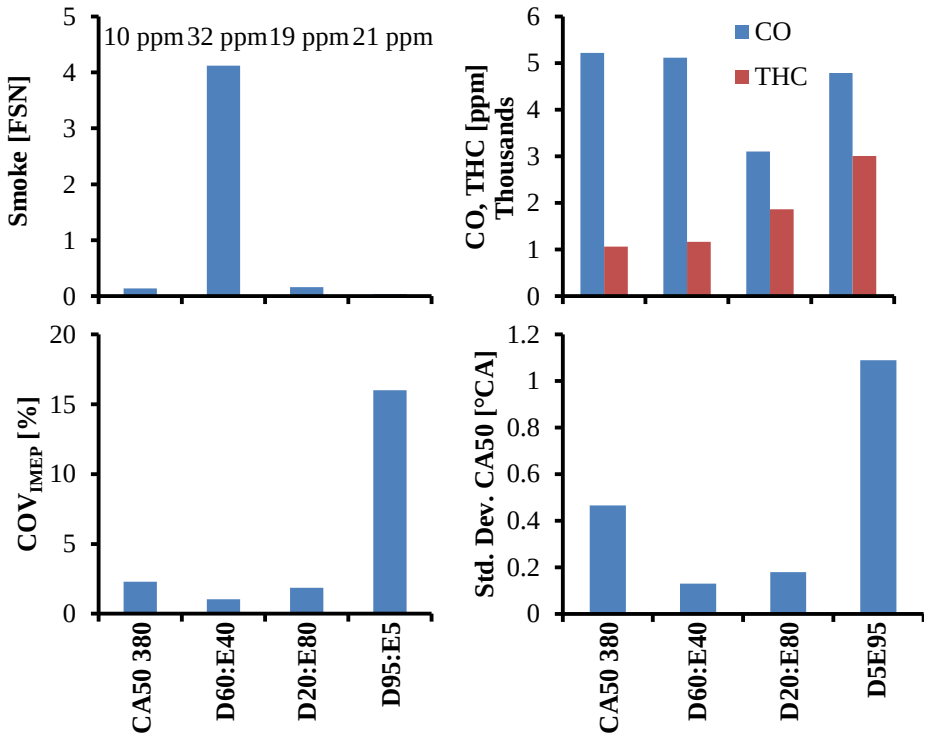

Figure 4-12 Comparison of Lowest NO_x Emission Results

4.3 Use of Micro Diesel Injection with Ethanol Port Injection

Reported in this section is the sensitivity of the injection timing of diesel direct injection on ethanol PFI and diesel DI dual fuel combustion. Two micro-injections tests (less than 5% diesel) and a D30:E70 test were conducted. The test conditions are shown in Table 4-9. The injection timing range of the micro-injection tests was limited to 2.5 °CA because if the injection timing was advanced further the $dp/d\theta_{max}$ became too high, and if the injection timing was further retarded the COV_{IMEP} was too high.

Table 4-9 Micro Diesel Injection with Ethanol Port Injection Test Conditions

	Diesel Micro	Diesel Micro	D30:E70
DI Inj. Timing [°CA]	350.0 – 352.5	355.0 – 357.5	356.0 – 364.0
DI Inj. Duration [µs]	255 - 260	270	400
DI Inj. Pressure [bar]	900	900	900
PFI Inj. Timing [°CA]	10	10	10
PFI Inj. Duration [µs]	5300	5300	4300
PFI Inj. Pressure [bar]	8	8	8
T_{Intake} [°C]	26	26	26
p_{Intake} [bar_{gauge}]	**1**	**0.5**	**1**
Engine Speed [rpm]	1500	1500	1500
Intake Oxygen [%]	20.7	20.7	20.7
IMEP [bar]	10.7 – 7.4	10.7 – 7.4	10.8 – 8.5
CA50 [°CA]	367.3 – 383.2	367.3 – 383.2	366.7 – 376.4

Shown in Figure 4-13 is the effect of injection timing on NO_x emissions for the three test conditions shown in Table 4-9. All conditions showed a reduction in NO_x emissions when injection timing was retarded. The NO_x reduction effect was more pronounced for the micro-injection tests, where a delay of 2.5 °CA resulted in a reduction of NO_x emissions of 220 ppm for the micro-injection test with an intake pressure of 1 bar_{gauge}. While the micro-injection test with an intake pressure of 0.5 bar_{gauge} test had a 990 ppm reduction in NO_x emissions. By comparison the D30:E70 test had a 500 ppm reduction in NO_x when the injection timing was retarded by 8 °CA.

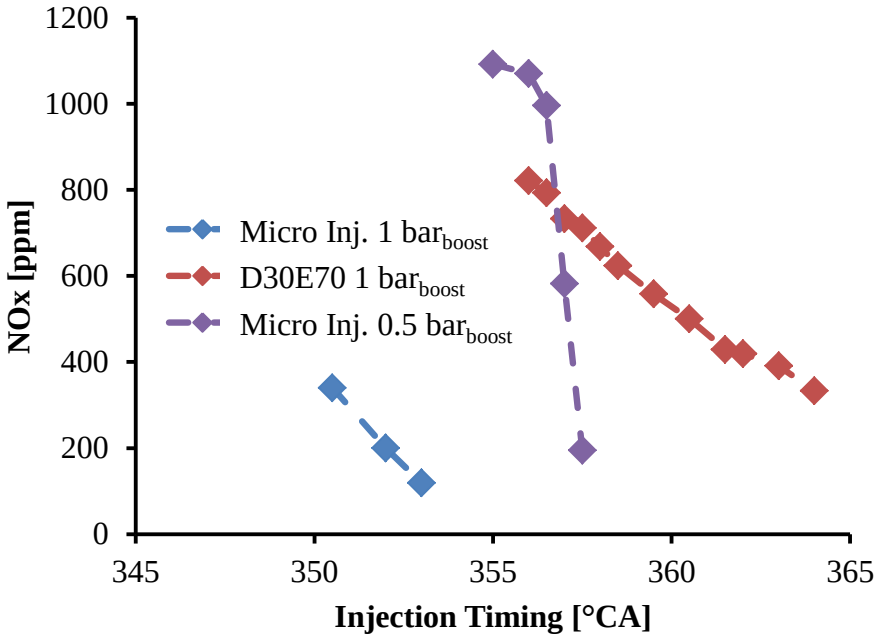

Figure 4-13 Effect of Micro Diesel Injection Timing on NO_x Emissions

Changing injection timings had minimal effect on smoke emissions as shown in Figure 4-14. The smoke emissions were less than 0.1 FSN for all conditions.

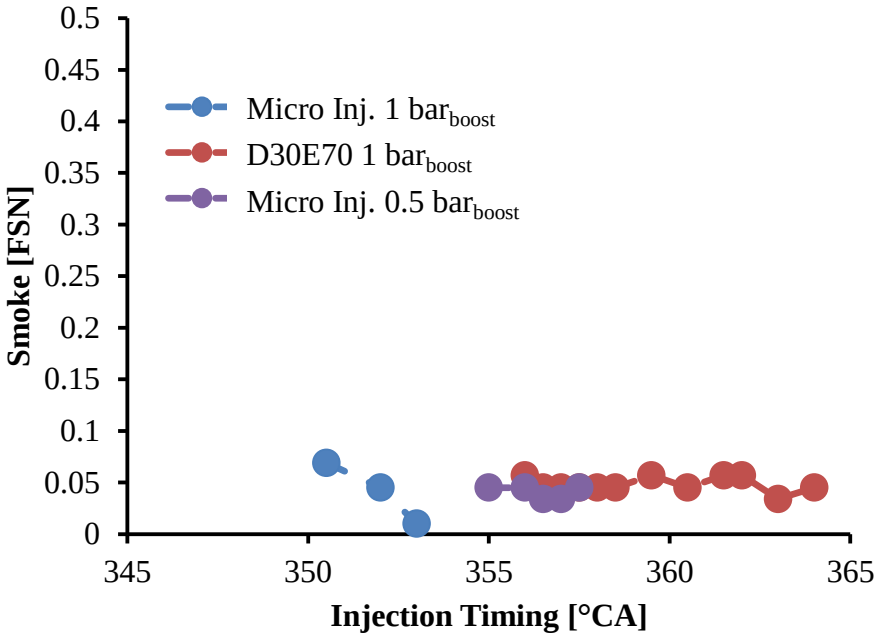

Figure 4-14 Effect of Micro Diesel Injection Timing on Soot Emissions

Shown in Figure 4-15 is the effect of diesel injection timing on IMEP. The IMEP was strongly effected by injection timing for the micro-injection tests. The 1 bar_{gauge} intake pressure test had a reduction in IMEP from 10.2 to 7.5 bar, while the micro-injection test with 0.5 bar_{gauge} intake pressure test had a drop from 10.7 to 7.4 bar IMEP when the injection timing is shifted by 2.5 °CA. The D30:E70 test had a drop from 10.8 to 8.5 IMEP when the injection timing was retarded by 8 °CA.

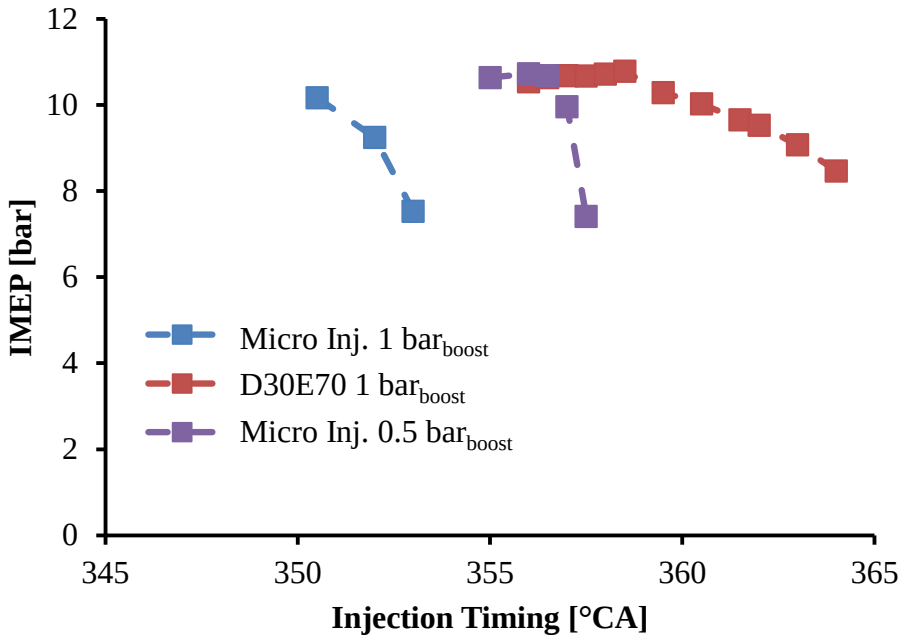

Figure 4-15 Effect of Micro Diesel Injection Timing on IMEP

Shown in Figure 4-16 is the effect of injection timing on the maximum pressure rise rate ($dp/d\theta$). All tests had a reduction in $dp/d\theta_{max}$ when the injection timing was delayed. For the micro-injection test with an intake pressure of 1 bar_{gauge} there was a reduction of 9.2 bar/°CA maximum pressure rise rate when the injection timing was retarded 2.5 °CA. Whereas, for the micro-injection test with an intake pressure of 0.5 bar_{gauge} there was a reduction in $dp/d\theta_{max}$ from 21.4 to 2.2 bar/°CA when the injection timing was retarded from 355 to 357.5 °CA. The D30:E70 had a reduction in the $dp/d\theta_{max}$ from 13.0 to 8.9 bar/°CA when the injection timing was shifted from 356 to 364 °CA.

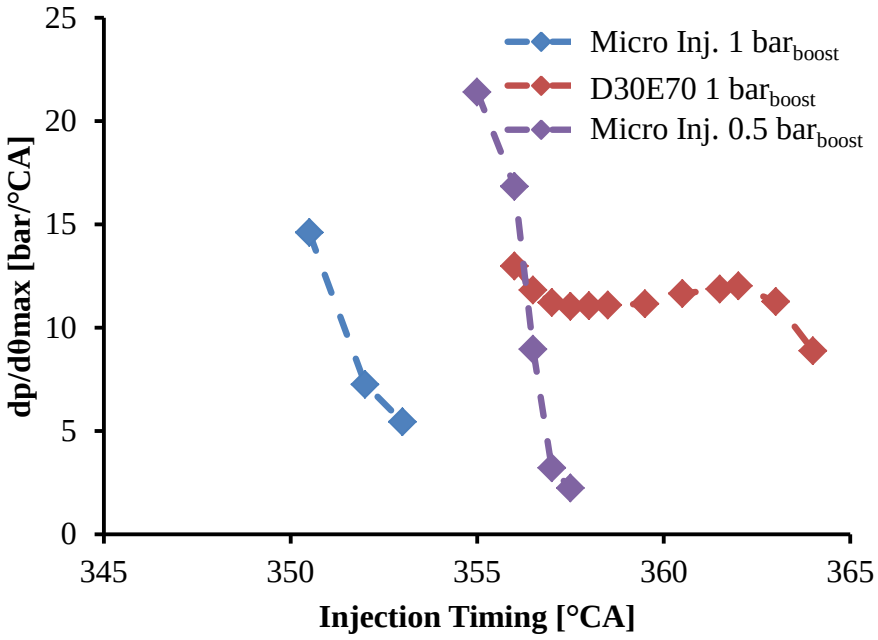

Figure 4-16 Effect of Injection Timing on Maximum Pressure Rise Rate

Illustrated in Figure 4-17 is the effect of the injection timing on the COV_{IMEP}. The COV_{IMEP} of the micro-injection tests is more sensitive to injection timing than the D30:E70 test. The COV_{IMEP} increased from 1.7% to 11.4% for the 1.0 bar_{gauge} intake pressure micro-injection test when the diesel injection timing was shifted by 2.5 °CA. While for the 0.5 bar_{gauge} intake pressure micro-injection test the COV_{IMEP} increased from 1% to 15.2% for the same shift in injection timing. Whereas the D30:E70 test had an increase in COV_{IMEP} from 1.2% to 2.3% when the diesel injection timing was retarded 8 °CA. Only the D30:E70 test remained below the 5% limit for the COV_{IMEP} for all injection timings used.

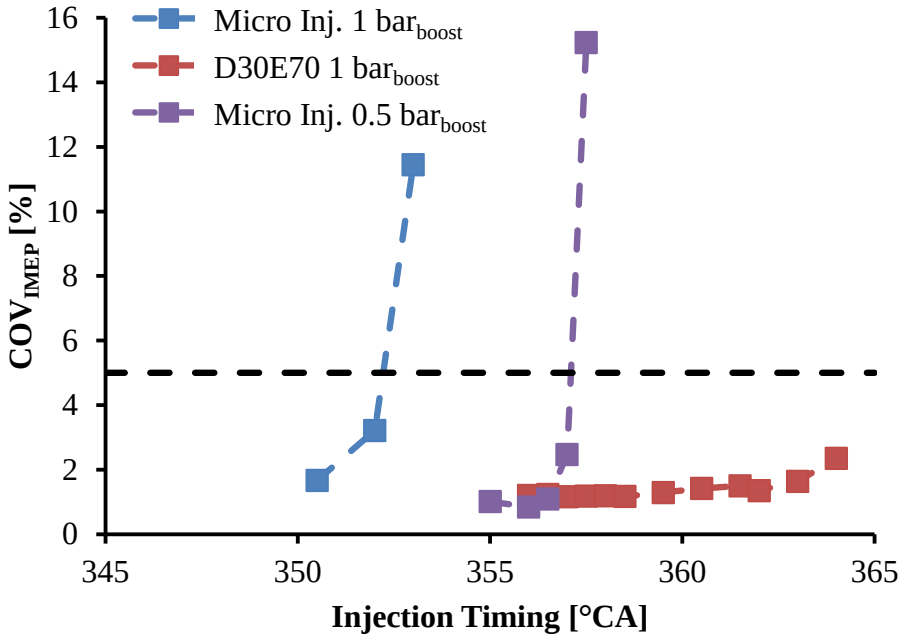

Figure 4-17 Effect of Micro Diesel Injection Timing on COV_{IMEP}

The effect of different injection timing on the standard deviation of CA50 is shown in Figure 4-18. The 1 bar_{gauge} micro-injection test had a decrease in the standard deviation of CA50 when the injection timing was shift from 350.5 to 352 °CA and then an increase when shifted from 352 to 353 °CA. The 0.5 bar_{gauge} micro-injection test had a continual increase in the standard deviation of CA50 with the delay of injection timing. The standard deviation of CA50 was greater than 0.5 °CA for both micro-injection tests when the average CA50 was 369 °CA or later. The D30:E70 test had a slight increase in the standard deviation of CA50 when the injection timing was retarded from 356 to 364 °CA. This means that the variation of COV_{IMEP} and the standard deviation of CA50 were more sensitive to injection timing when the diesel – ethanol ratio was less than 5%.

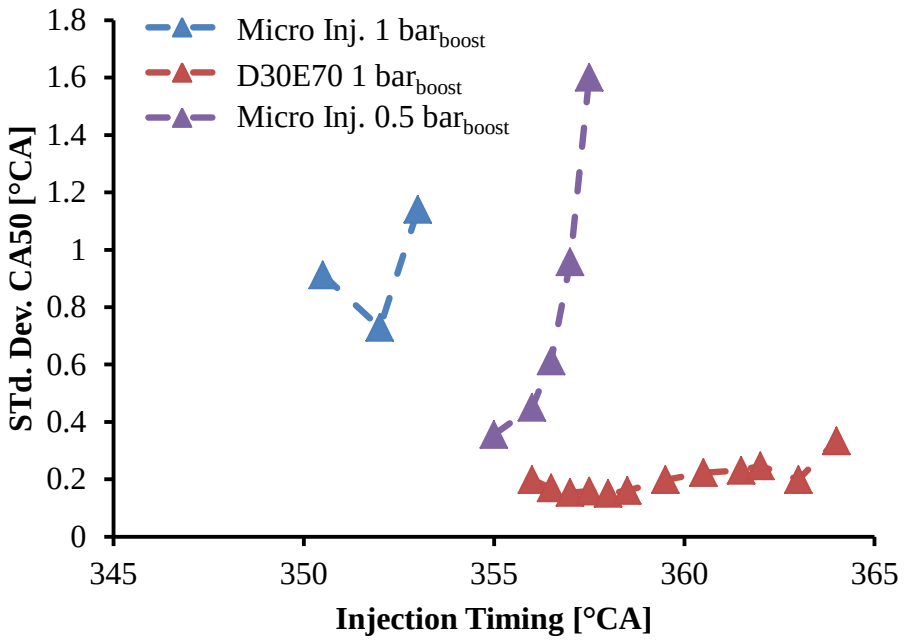

Figure 4-18 Effect of Micro Diesel Injection Timing on Std. Dev. CA50

Shown in Figure 4-19 to Figure 4-24 are the 200 consecutive cycle traces of pressure and HRR for the earliest and latest injection timings of each of the three tests. The earliest and latest timings are used as a comparison between the lowest and highest combustion instability in terms of COV_{IMEP}.

Illustrated in Figure 4-19 are the pressure and heat release traces for the earliest injection timing of 350.5 °CA of the micro-injection test with an intake pressure of 1.0 bar_{gauge}. The mean, minimum, maximum, and variation of the combustion parameters are shown in Table 4-10. Even though the COV_{IMEP} was 1.7% there is more variation in the pressure and HRR curves than seen in Figure 4-10 where the COV_{IMEP} was 1.6%. The wider distribution of the 200 cycle pressure and HRR could be caused by the lower intake pressure resulting in a lower peak pressure and temperature. However, this increased variation was not reflected by the COV_{IMEP}, further investigation of this phenomena is required. There was a two peak heat release shape, with the second peak significantly greater than the first, a reason for this could be the first peak was the combustion of the diesel fuel while the second peak was the propagation of the flame through the cylinder. Another possible cause could be the combustion of the diesel fuel caused an increase in the in-cylinder temperature which resulted in auto-ignition of the remaining fuel in the cylinder.

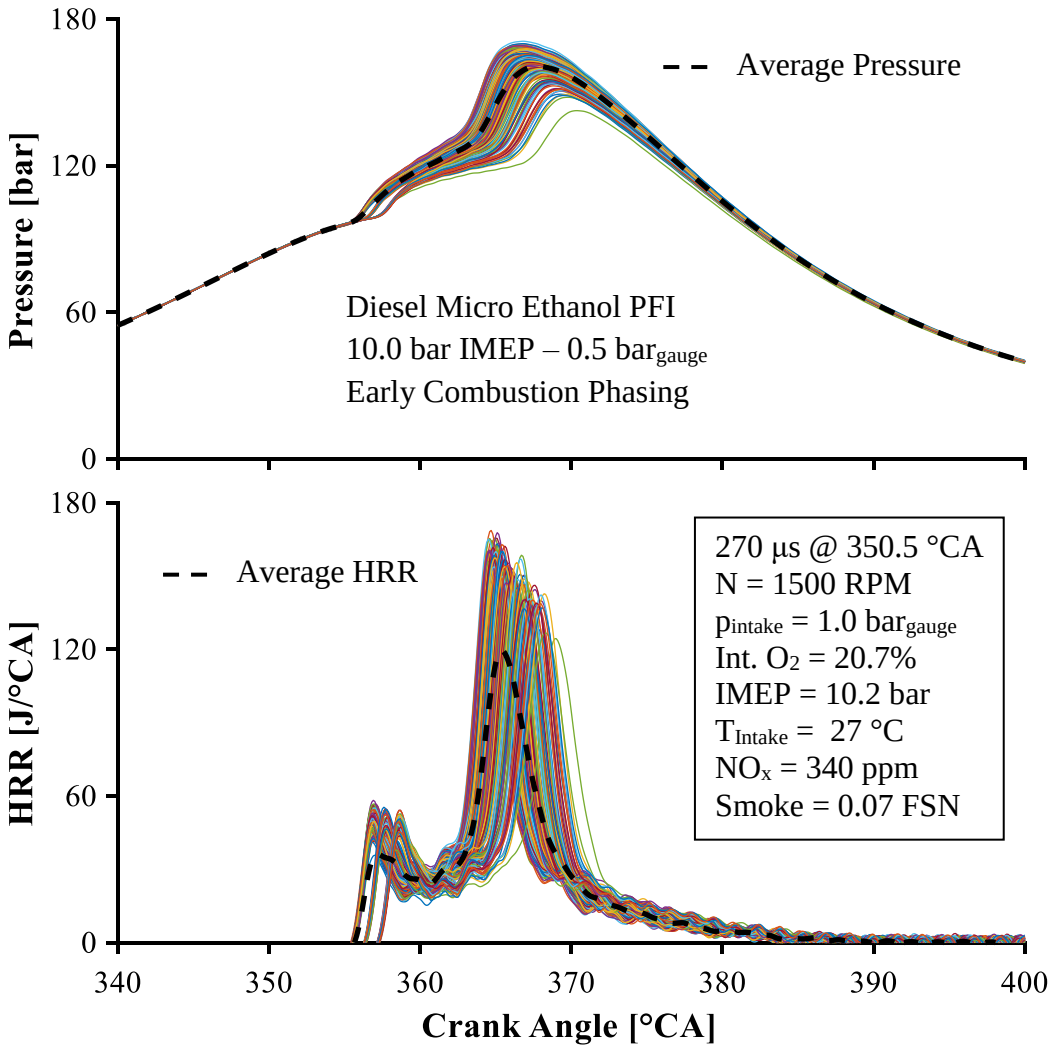

Figure 4-19 200 Cycle Pressure and HRR Trace for Diesel Micro Injection : Early SOI

Table 4-10 Combustion Parameters of Early Micro-Inj. at 1.0 bar_g 200 Cycle Data

Parameter	Mean	Minimum	Maximum	Variation
p_{max}	162.0 bar	142.5 bar	170.9 bar	3.2%
IMEP	10.2 bar	9.4 bar	10.6 bar	1.7%
CA50	365.7 °CA	364.4 °CA	368.8 °CA	0.91 °CA

Shown in Figure 4-20 are the 200 consecutive cycle traces of the pressure and HRR for the 1.0 bar intake pressure test with an injection timing of 353 °CA. The mean, minimum, maximum, and variation of the combustion parameters are shown in Table 4-11. Greater variation can be seen in the pressure and heat release traces than in Figure 4-19, this is reflected in the high COV_{IMEP} and standard deviation of CA50. The most significant variation occurs around the second peak of heat release which is later than in the expansion stroke than in Figure 4-19. The large variation in HRR during the second peak could be because the pressure and temperature are reduced due to the expanded combustion volume, resulting in the flame not propagating through the whole cylinder. Another possible reason could be variation in the mixing of the diesel injection with the ethanol and air mixture, causing variations in the peak temperature and pressure.

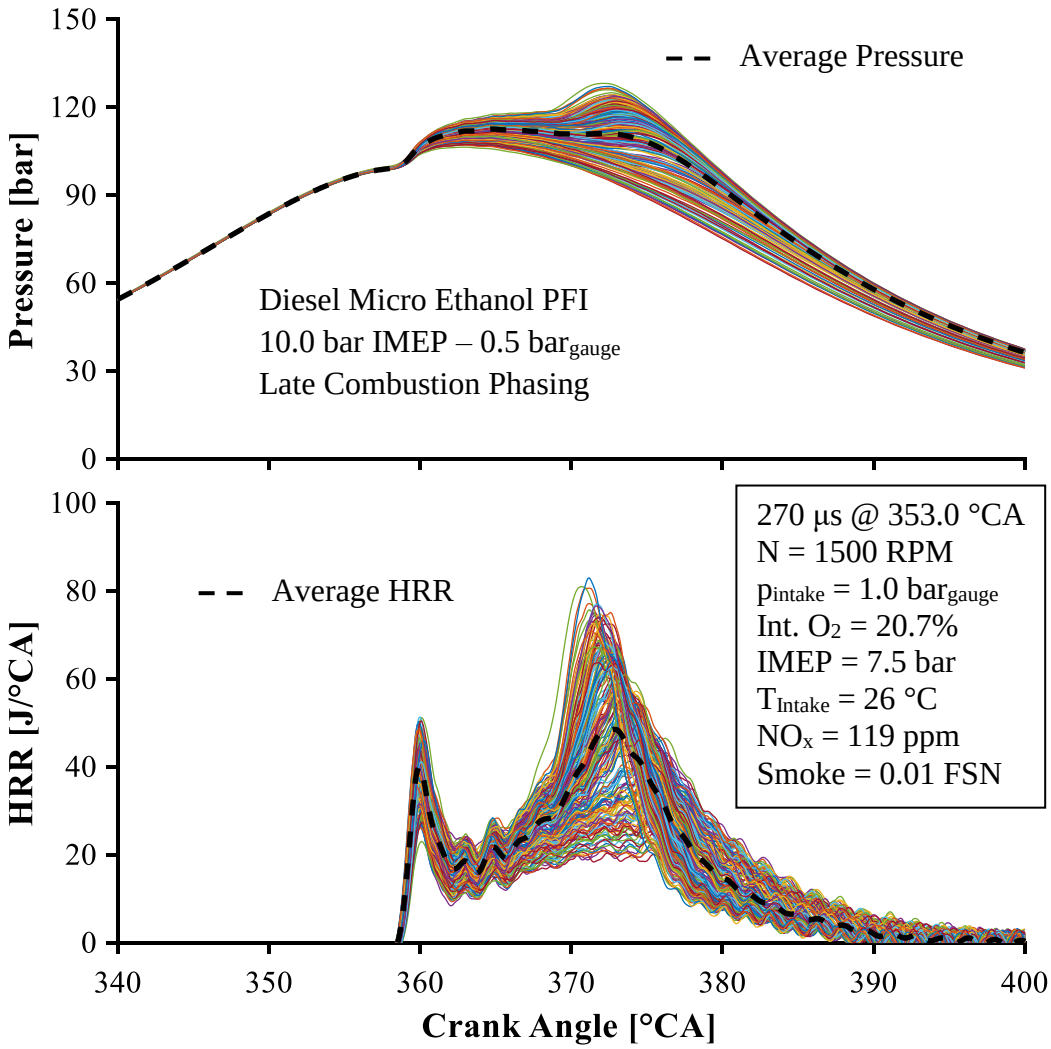

Figure 4-20 200 Cycle Pressure and HRR Trace for Diesel Micro Injection : Late SOI

Table 4-11 Combustion Parameters of Late Micro-Inj. at 1.0 bar_g 200 Cycle Data

Parameter	Mean	Minimum	Maximum	Variation
p_{max}	112.5 bar	106.3 bar	128.0 bar	4.4%
IMEP	7.5 bar	4.5 bar	8.5 bar	11.4%
CA50	372.1 °CA	370.1 °CA	374.5 °CA	1.14 °CA

Shown in Figure 4-21 are the pressure and HRR traces for the 0.5 bar_{gauge} intake pressure micro-injection test with an injection timing of 355 °CA. The mean, minimum, maximum, and variation of the combustion parameters are shown in Table 4-12. The pressure and HRR traces have a similar shape to Figure 4-19, however there is less variation between the minimum and maximum p_{max} of the 200 cycles. Additionally the HRR trace has reduced temporal variance at the highest HRR. The combustion was more rapid than seen in Figure 4-19 and had a much higher peak HRR, which resulted in a higher peak cylinder temperature and therefore produced more NO_x emissions.

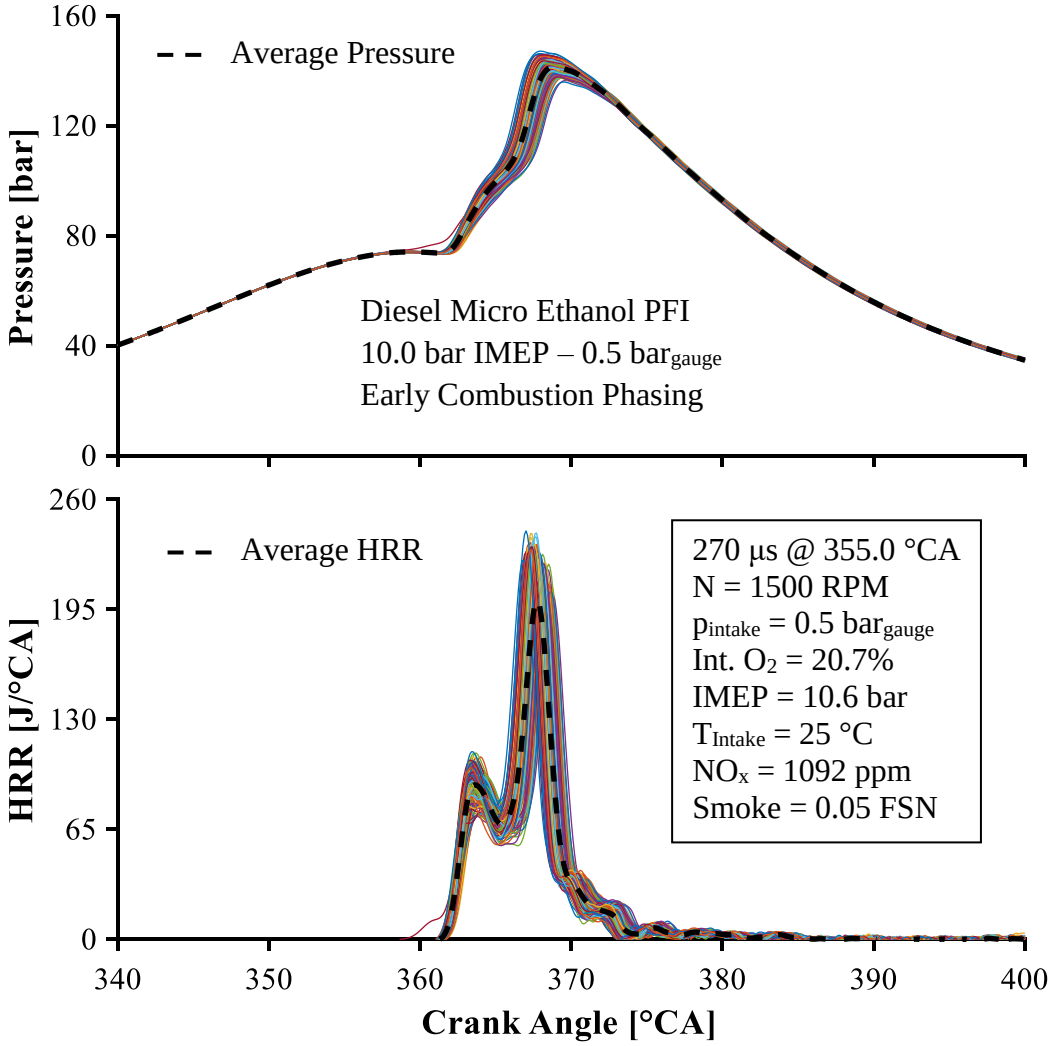

Figure 4-21 200 Cycle Pressure and HRR Trace for Diesel Micro Injection : Early SOI

Table 4-12 Combustion Parameters of Early Micro-Inj. at 0.5 bar_g 200 Cycle Data

Parameter	Mean	Minimum	Maximum	Variation
p_{max}	141.9 bar	135.9 bar	147.1 bar	1.0%
IMEP	10.6 bar	10.2 bar	10.9 bar	1.5%
CA50	367.3 °CA	366.5 °CA	368.3 °CA	0.36 °CA

Shown in Figure 4-22 are the pressure and HRR traces for the 0.5 bar_{gauge} intake pressure micro-injection test with an injection timing of 357.5 °CA. This test condition had the greatest COV_{IMEP} and standard deviation of CA50 of the injection timing tests. The mean, minimum, maximum, and variation of the combustion parameters are shown in Table 4-13. Some of the pressure traces were barely greater than the motoring pressure and the peak HRR was as low as 10 J/°CA for some cycles, this is similar to Figure 4-11. The combustion duration was also the longest of the injection timing tests, extending beyond 400 °CA. However, due to the low HRR and p_{max} the in-cylinder temperature was low, resulting in low NO_x emissions.

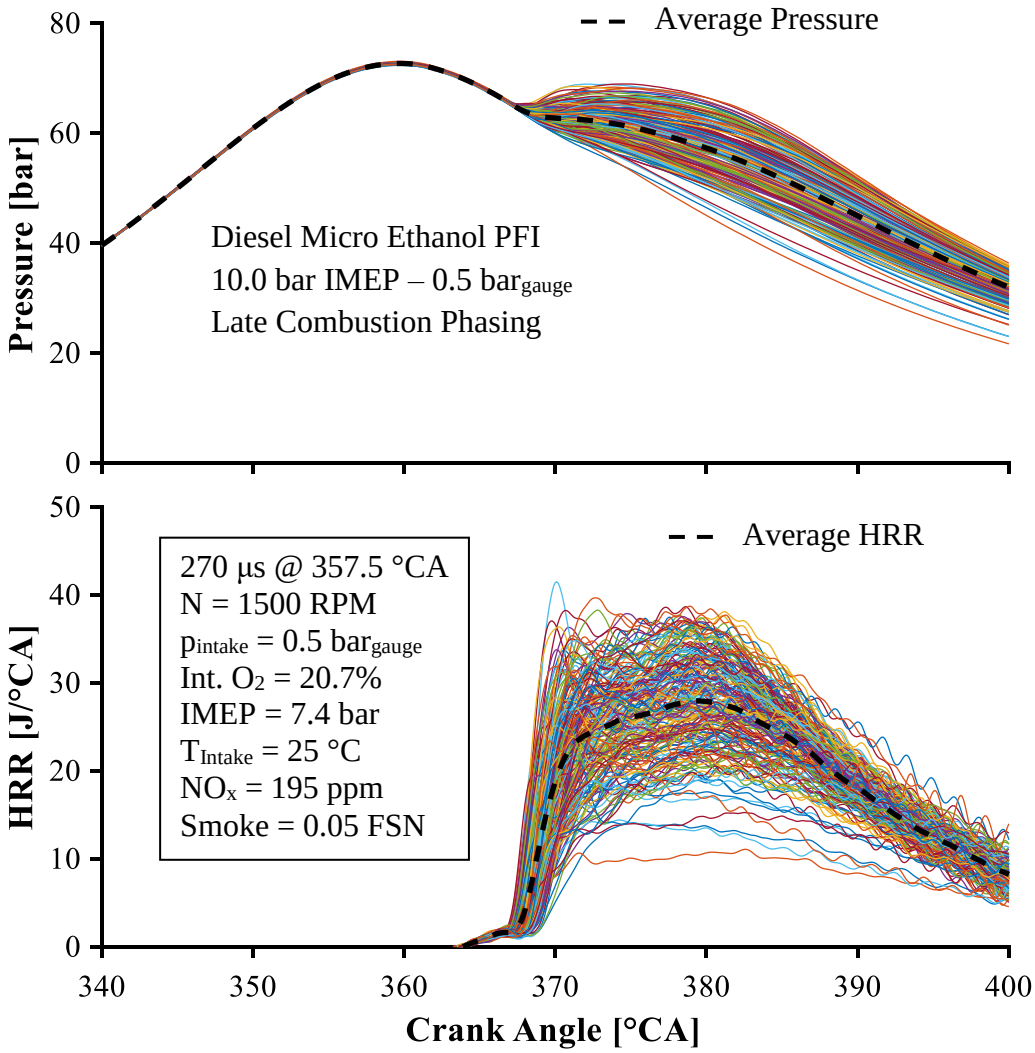

Figure 4-22 200 Cycle Pressure and HRR Trace Diesel Micro Injection : Late SOI

Table 4-13 Combustion Parameters of Late Micro-Inj. at 0.5 bar_g 200 Cycle Data

Parameter	Mean	Minimum	Maximum	Variation
p_{max}	63.1 bar	60.1 bar	68.9 bar	3.2%
IMEP	7.4 bar	2.7 bar	9.1 bar	15.2%
CA50	383.2 °CA	379.9 °CA	387.1 °CA	1.60 °CA

Shown in Figure 4-23 are the pressure and HRR traces for the D30:E70 test with an injection timing of 356 °CA. The mean, minimum, maximum, and variation of the combustion parameters are shown in Table 4-14. The pressure and HRR traces were similar to Figure 4-8, and had less variation than the previous four cases. There was a dual peak HRR shape with the second peak being much larger than the first. Therefore, the majority of the combustion occurred in the diffusion combustion mode, resulting in over 800 ppm NO_x emissions.

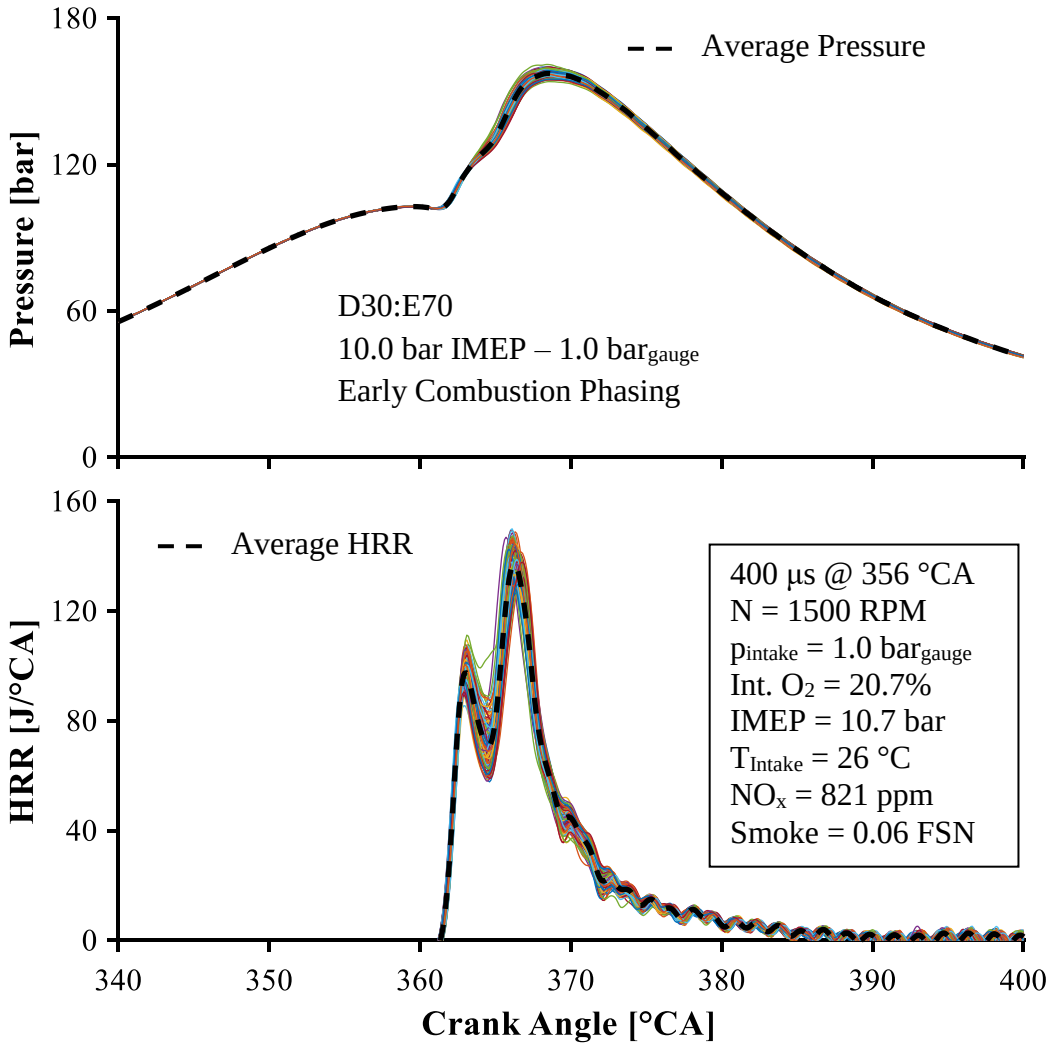

Figure 4-23 200 Cycle Pressure and HRR Trace for D30:E70 : Early SOI

Table 4-14 Combustion Parameters of Early Inj. Timing for D30:E70 200 Cycle Data

Parameter	Mean	Minimum	Maximum	Variation
p_{max}	140.2 bar	137.1 bar	144.9 bar	0.8%
IMEP	10.5 bar	10.2 bar	10.9 bar	1.2%
CA50	369.7 °CA	369.1 °CA	370.2 °CA	0.16 °CA

Shown in Figure 4-24 are the pressure and HRR traces for the D30:E70 diesel-ethanol ratio with an injection timing of 364 °CA. The mean, minimum, maximum, and variation of the combustion parameters are shown in

Table 4-15. There was more variation in both the pressure and HRR traces when injection was retarded, as seen by the increased difference between the minimum and maximum IMEP and p_{max}. When the injection timing was 356 °CA the difference was 7.8 bar for the p_{max} and 0.7 bar for the IMEP, however when the injection was retarded to 364 °CA the difference in p_{max} increased to 9.6 bar and the difference in IMEP increased to 1.1 bar. At this injection timing the two peaks of heat release have merged together, however as there was a high peak of HRR the in-cylinder temperature is above the NO_x production threshold, resulting in over 300 ppm NO_x emission.

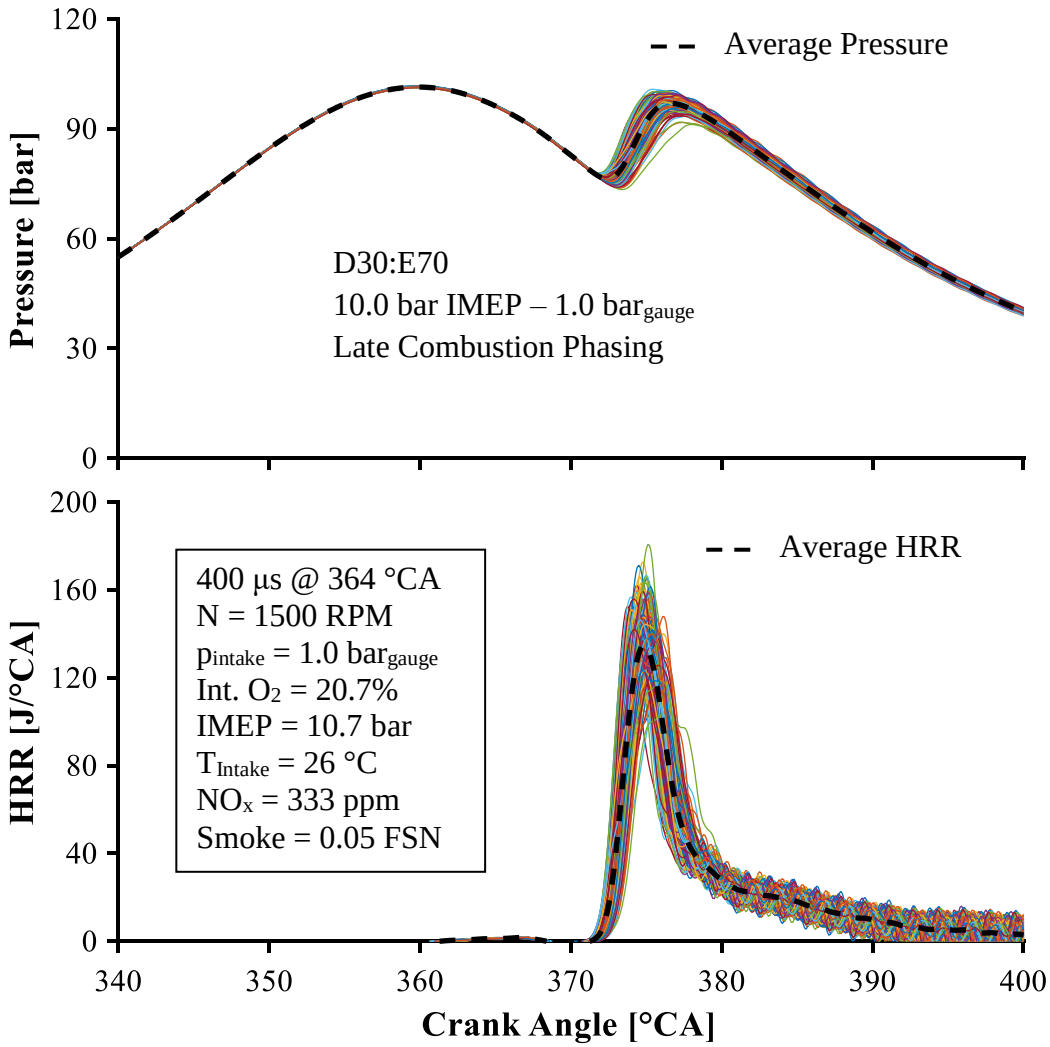

Figure 4-24 200 Cycle Pressure and HRR Trace for D30:E70 : Late SOI

Table 4-15 Combustion Parameters of Late Inj. Timing for D30:E70 200 Cycle Data

Parameter	Mean	Minimum	Maximum	Variation
p_{max}	97.0 bar	91.2 bar	100.8 bar	1.7%
IMEP	8.5 bar	7.9 bar	9.0 bar	2.3%
CA50	376.4 °CA	375.8 °CA	377.8 °CA	0.16 °CA

From the results presented in this section it was shown that when the diesel to ethanol ratio is reduced to the point where the diesel injection by itself does not produce positive IMEP at idle conditions, the combustion is sensitive to injection timing and the cycle-to-cycle variation increases.

4.4 Chapter Summary

The effect of diesel – ethanol ratio on emissions, load, and combustion stability was presented. The influence of EGR on D100:E0 to D5:E95 was presented as well as the effect of injection timing on micro-injection diesel ignited ethanol.

A decrease in NO_x and soot emissions was observed when the diesel – ethanol ratio was decreased.

EGR was effective at reducing NO_x for all test conditions, however, for the tests using ethanol ratios of 80% and greater, there was no increase in PM emissions with the decrease of intake oxygen concentration. Therefore, it is possible to avoid the NO_x – soot trade off if a large quantity of ethanol is used.

COV_{IMEP} only exceeded the 5% limit for three test conditions all of which had a diesel – ethanol ratio greater than 95% ethanol, this means that the implementation of a vehicle primarily fueled by ethanol with a small direct injection of diesel for ignition control could be problematic. The primary problem that would need to be resolved would be to determine if the high cycle-to-cycle variations occur within the required operating range of the engine, if they do then an adjustment of the fueling strategy is necessary at these conditions. The diesel only case had the largest variation of COV_{IMEP} values without showing any clear correlation to EGR. The majority of COV_{IMEP} values obtained were less than 1% when the

intake oxygen concentration was reduced from 19% to 12%. With the increasing ethanol ratio there was an increase in COV_{IMEP} for the majority of intake oxygen concentrations tested. For the EGR tests the 5% limit for the COV_{IMEP} was only exceed when the D5:E95 test had an intake oxygen concentration less than 13.7%.

The standard deviation of CA50 increased with the increase of ethanol fraction. EGR had minimal effect on the standard deviation of CA50 for the diesel only case, while for the D80:E20, D60:E40, and D40:E60 tests there was an approximately linear increase in the standard deviation of CA50 with the decrease in intake oxygen. The D20:E80 and D5:E95 tests both had an exponential increase in the standard deviation of CA50 with increasing EGR, however it was much more pronounced in the D5:E95 case, especially below 15% intake oxygen concentration.

When the diesel injection was reduced to the shortest possible duration while maintaining reliable ignition, 270 μs at 900 bar injection pressure, the combustion stability becomes sensitive to injection timing. When the injection timing was retarded by 2.5 °CA there was a significant reduction in NO_x, IMEP, and $dp/d\theta_{max}$ for intake pressures of 0.5 and 1.0 bar_{gauge}. However, retarding the injection timing resulted in increased cycle-to-cycle variation. The COV_{IMEP} of the diesel-micro injection with 1.0 bar_{gauge} intake pressure increases from 1.7% to 11.4% when the injection timing was retarded 2.5 °CA. While for the 0.5 bar_{gauge} tests the COV_{IMEP} increased from 1.0% to 15.2% for the same shift in injection timing. The standard deviation of CA50 increases by 0.2 °CA for the 1.0 bar_{gauge} test when injection was moved from 350.5 to 353 °CA, whereas for the 0.5 bar_{gauge} test it increased from 0.4 to 1.6 °CA when the injection was moved from 355 to 357.5 °CA.

CHAPTER 5: CONCLUSIONS AND FUTURE RECOMMENDATIONS

Presented in this chapter are the concluding remarks of this work and recommendations of future work.

5.1 Conclusions

Exhaust gas recirculation was found to effectively reduce NO_x emissions for all single shot diesel test conditions investigated. For three of the five single shot diesel test conditions this came at the expense of a continual increase in smoke emissions. The 3.5 bar IMEP and 10 bar IMEP 380 °CA CA50 tests were able to achieve simultaneous reduction of smoke and NO_x emission. However, only the 10 bar test was able to reach low temperature combustion identified by simultaneous ultra-low NO_x and soot emissions. The use of exhaust gas recirculation decreased combustion efficiency signified by an increase in CO and THC emissions, and at intake oxygen concentrations less than 13% resulted in a loss of load for the 10 bar IMEP tests.

For the 3.5 bar and 6.1 bar IMEP tests, the COV_{IMEP} of the 3.5 bar test was greater than the 6.1 bar test for all intake oxygens. Additionally there was a slight increase in the COV_{IMEP} when intake oxygen was reduced to approximately 13%, at which point the 6.1 bar test was stopped due to excessively high smoke. Whereas the intake oxygen of 3.5 bar test was further reduced to 10.5%, during which there was an exponential increase in the COV_{IMEP}. These results agree with those found in literature [14 and 17].

Whereas, the 10 bar IMEP tests had conflicting results to those found in literature [14 and 17]. With decreasing oxygen there appeared to be a reduction in the COV_{IMEP} for the tests with a CA50 of 366 and 369 °CA, while the CA50 380 °CA case had minimal change in the COV_{IMEP} with increased exhaust gas recirculation. A possible explanation for the

contrary results to literature is that there are fluctuations or oscillations in the variation of combustion over a large number of cycles such as found be Sen et al. [18].

It was also possible to reduce peak NO_x and soot emissions by retarding combustion phasing. With the retardation of CA50 from 366 to 380 °CA there was a reduction of peak NO_x emissions from 286 to 75 ppm, and a reduction of peak smoke production from 4.96 to 1.87 FSN. However, the excessive retarding of combustion phasing resulted in an increase of incomplete combustion products, CO and THC, for the same intake oxygen concentration. Retarding the combustion phasing resulted in no correlation between the intake oxygen concentration and the COV_{IMEP}. For the CA50 of 366 and 369 °CA tests, there was a gradual linear increase in the standard deviation of CA50 with increasing EGR, an approximate increase of 20%. There was a greater effect of reducing intake oxygen on the standard deviation of CA50 for the 380 °CA CA50 test, where there was an increase of approximately 70%.

When ethanol fuel was used in combination with diesel there was a decrease in NO_x and PM emissions. EGR was effective at further reducing NO_x for all diesel – ethanol ratios investigated in this work. When a diesel – ethanol ratio less than 20% was used there is no increase in smoke emissions with a decrease of intake oxygen concentration.

The reduction of intake oxygen concentration did not have a significant effect on the COV_{IMEP} for the majority of the diesel – ethanol ratio tests. When the intake oxygen concentration was reduced to 13.7% the COV_{IMEP} of the D5:E95 test abruptly increased to 16%.

The standard deviation of CA50 increased with the increase of ethanol fraction. EGR had minimal effect on the standard deviation of CA50 for the D100:E0 test. While for the

D80:E20, D60:E40 and D40:E60 cases there was a linear increase in the standard deviation of CA50 with a decrease in intake oxygen concentration. The D20:E80 and D5:E95 tests had a linear increase in the variation of CA50 until approximately 15% intake when there was an exponential increase.

The emission production and combustion stability of a diesel micro-injection used to ignite a mixture of ethanol and air was found to be sensitive to injection timing. The retardation of the diesel micro-injection by 2.5 °CA resulted in a 220 ppm and 990 ppm reduction in NO_x at intake pressures of 1.0 and 0.5 bar_{gauge} respectively. This 2.5 °CA shift in injection timing also caused a 2.6 bar reduction in the IMEP and a 9.2 bar/°CA reduction in the maximum pressure rise rate for the 1.0 bar_{gauge} test. For the 0.5 bar_{gauge} tests there was a reduction of 3.2 bar IMEP and 19.2 bar/°CA $dp/d\theta_{max}$ for the same change of injection timing. The COV_{IMEP} increased exponentially for both intake pressures with the 2.5 °CA delay in injection timing. The COV_{IMEP} increased by 9.7% and 14.2% for the 1.0 bar_{gauge} and 0.5 bar_{gauge} tests respectively when the injection timing was retarded. The standard deviation of the 1.0 bar_{gauge} test increased by 0.2 °CA, while the 0.5 bar_{gauge} tests increased from 0.4 to 1.6 °CA when injection timing was shifted 2.5 °CA.

From the tests conducted it was found that:

1. The application of EGR did not have a significant effect on the COV_{IMEP} of diesel only combustion
2. The application of EGR increased the standard deviation of CA50 of diesel only combustion
3. The retarding of CA50 to 380 °CA reduced the COV_{IMEP} of diesel only combustion

4. The retarding of CA50 to 380 °CA increased the standard deviation of CA50 of diesel only combustion
5. Decreasing the diesel – ethanol ratio to 5% did not have a significant effect the COV_{IMEP} for intake oxygen concentrations greater than 14%
6. The application of EGR did not have a significant effect on COV_{IMEP} of diesel – ethanol ratios greater than 20%
7. Decreasing the diesel – ethanol ratio increased the standard deviation of CA50
8. The application of EGR increased the standard deviation of CA50 for all diesel – ethanol ratios
9. Retarding the injection timing of micro-injection diesel with ethanol port injection increased the COV_{IMEP}
10. Retarding the injection timing of micro-injection diesel with ethanol port injection increased the standard deviation of CA50

5.2 Future Recommendations

If future work on this topic is to be conducted it is recommended to investigate the effect of each cycle on the proceeding cycle as well as pattern and regression analysis. The pattern analysis could determine if the combustion stability is going to degrade or improve if the control parameters were left unchanged. Another recommendation is to check the repeatability of the cycle-to-cycle variation measurements by repeating the test conditions and recording a larger amount of consecutive cycles to mitigate any outliers and determine if there are low frequency oscillations in the variation of combustion over time.

REFERENCES

1. U.S. Department of Transportation, "National Transport Statistics 2016", https://www.rita.dot.gov/bts/sites/rita.dot.gov.bts/files/publications/national_transportation_statistics/index.html, February 2016 (accessed)
2. U.S. Energy Information Administration, "Annual Energy Outlook 2015 with projections to 2040", www.eia.gov/outlooks/aeo/pdf/0383(2015).pdf, February 2016 (accessed)
3. Environmental Protection Agency, "U.S. Greenhouse Gas Inventory Report: 1990-2014", http://www.epa.gov/climatechange/ghgemissions/usinventoryreport.html, February 2016 (accessed)
4. Environmental Protection Agency, Department of Transportation, "Greenhouse Gas Emissions and Fuel Efficiency Standard for Medium- and Heavy Duty Engines and Vehicles – Phase 2", https://www.gpo.gov/fdsys/pkg/FR-2016-10-25/pdf/2016-21203.pdf, November 2017 (accessed)
5. Dieselnet, "Summary of Emission Limits", https://www.dieselnet.com/standards/us/hd.php, February 2016 (accessed)
6. Ogawa, H., Li, T., Miyamoto, N., "Characteristics of low temperature and low oxygen diesel combustion with ultra-high exhaust gas recirculation", International Journal of Engine Research, 2007 8:365, 2007
7. Akihama, K., Takatori, Y., Inagaki, K., Sasaki, S., Dean, A., "Mechanism of Smokeless Rich Diesel Combustion by Reducing Temperature", SAE Technical Paper 2001-01-0655, 2001

8. Jacobs, T., Assanis, “The attainment of premixed compression ignition low-temperature combustion in a compression ignition direct injection engine”, Proceedings of the Combustion Institute, vol. 31, no. 2, pp. 2913 – 2920, 2007
9. Reitz, R., “Directions in internal combustion research”, Combustion and Flame 160: 1-8, 2013
10. Han, X., Tjong, J., Wang, M., Reader, G., Zheng, M., “Renewable Ethanol use for Enabling High Load Clean Combustion in a Diesel Engine”, SAE Technical Paper, 2013-01-0904, 2013
11. Asad, U., Kumar, R., Zheng, M., Tjong, J., “Ethanol – fueled low temperature combustion: a pathway to clean and efficient diesel engine cycles”, Applied Energy 157: 838 – 850, 2015
12. Gao, T., Yu, S., Li, T., Zheng., M, “Impact of multiple pilot diesel injections on the premixed combustion of ethanol fuel” Proceedings of the Institution of Mechanical Engineers, Part D: Journal of Automobile Engineering, 2017
13. Heywood, J., “Internal Combustion Engine Fundamentals”, McGraw-Hill, New York, 1988
14. Kyrtatos, P., Hoyer, K., Obrecht, P., Boulouchos, K., “Apparent effects of in-cylinder pressure oscillations and cycle-to-cycle variability on heat release rate and soot concentration under long ignition delay conditions in diesel engines”, International Journal of Engine Research, Vol. 15 (3), 325 – 337, 2014
15. Maurya, R., Agarwal, A., “Experimental investigation on the effect of intake air temperature and air-fuel ratio on cycle-to-cycle variations of HCCI combustion and performance parameters”, Journal of Applied Energy, 88: 1153 – 1163, 2011

16. Koizumi, I., Gyakushi, N., Takamoto, Y., 'Study on the Cycle-by-Cycle Variation in Diesel Engines', Bulletin of the JSME, Vol. 20, No. 145, Paper No. 145-14, 1977
17. Kyrtatos, P., Brückner, C., Boulouchos, K., "Cycle-to-cycle variations in diesel engines", Journal of Applied Energy, 171: 120 – 132, 2016
18. Sen, A., Longwic, R., Litak, G., Górski, K., "Analysis of cycle-to-cycle pressure oscillations in a diesel engine", Journal of Mechanical Systems and Signal Processing, 22: 362 – 373, 2008
19. Wang, Y., Xiao, F., Zhao, Y., Li, D., Lei, X., "Study on cycle-by-cycle variations in a diesel engine with dimethyl ether as port premixing fuel", Journal of Applied Energy, 143: 58 – 70, 2015
20. Ali, O., Mamat, R., Masjuki, H., Abdullah, A., "Analysis of blended fuel properties and cycle-to-cycle variation in a diesel engine with a diethyl ether additive", Journal of Energy Conversion and Management, 108: 511 – 519, 2016
21. Asad, U., Kumar, R., Han, X., Zheng, M., "Precise instrumentation of a diesel single-cylinder research engine", Journal of the International Measurement Confederation, 44: 1261 – 1278, 2011
22. Asad, U., "Advanced Diagnostics, Control, and Testing of Diesel Low Temperature Combustion", Ph.D. Dissertation, 2009
23. Divekar, P., "Clean Combustion Control in a Compression Ignition Engine:, Ph.D. Dissertation, 2016
24. Zheng, M., Reader, G., Hawley, J., "Diesel engine exhaust gas recirculation – a review on advanced and novel concepts", Journal of Energy Conversion and Management, 45: 883 – 900, 2004

25. Bryden, G., Divekar, P., Yang Z., and Zheng M., “Ignition delay, heat release profile, and emission correlation in diesel low temperature combustion” Combustion Institute Canadian Section - May 2015

LIST OF PUBLICATIONS

Refereed Journals

1. Yanai, T., **Bryden, G**., Dev, S., Reader, G. T., Zheng, M., "Investigation of ignition characteristics and performance of a neat n-butanol direct injection compression ignition engine at low load" – Fuel 208C, pp 137-148, 2017.

Refereed Conference Proceedings

1. Xie, K., Yu, S., Yu, X., **Bryden, G**. et al., "Investigation of Multi-Pole Spark Ignition Under Lean Conditions and with EGR" - SAE Technical Paper 2017-01-0679 – April 2017.
2. Gao, T., Jeftic, M., **Bryden, G.,** Reader, G. et al.,"Heat Release Analysis of Clean Combustion with Ethanol Ignited by Diesel in a High Compression Ratio Engine" - SAE Technical Paper 2016-01-0766 – April 2016.

Non-Refereed Conference Proceedings

1. **Bryden, G.**, Divekar, P., Yang Z., and Zheng M., "Ignition delay, heat release profile, and emission correlation in diesel low temperature combustion" Combustion Institute Canadian Section - May 2015.
2. **Bryden, G.**, Aversa, C., Divekar, P., and Zheng M., "Preliminary Investigation of the Influence of Low Temperature Combustion on Diesel Engine Heat Release Profiles" Combustion Institute Canadian Section - May 2013.

VITA AUCTORIS

NAME:	Geraint Bryden
PLACE OF BIRTH:	Great Barton, Suffolk, England
YEAR OF BIRTH:	1991
EDUCATION:	B.ASc Mechanical Engineering University of Windsor 2009 – 2014
	M.ASc Mechanical Engineering University of Windsor 2014 - 2017